ISSN Application No, 21816

Indian Journal of Automotive Technology

Volume No. 8

Issue No. 2

May - August 2025

ENRICHED PUBLICATIONS PVT. LTD

S-9, IInd FLOOR, MLU POCKET,
MANISH ABHINAV PLAZA-II, ABOVE FEDERAL BANK,
PLOT NO-5, SECTOR-5, DWARKA, NEW DELHI, INDIA-110075,
PHONE: - + (91)-(11)-47026006

ISSN Application No, 21816

Indian Journal of Automotive Technology

Aims and Scope

Indian Journal of Automotive Technology published by Enriched Publications publishes original research in all fields of AUTOMOTIVE TECHNOLOGY, SCIENCE and ENGINEERING. It fosters thus the exchange of ideas among researchers in different parts of the world and also among researchers who emphasize different aspects of the foundations and applications of the field.

The Journal, by providing an right medium of communication, is encouraging this growth and is encompassing all aspects of the field from thermal engineering, flow analysis, structural analysis, modal analysis, control, vehicular electronics, mechatronics, electro-mechanical engineering, optimum design methods, ITS, and recycling. Interest extends from the basic science to technology applications with analytical, experimental and numerical studies.

When outstanding advances are made in existing areas or when new areas have been developed to a definitive stage, special review articles will be considered by the editors.

ISSN Application No, 21816

Indian Journal of Automotive Technology

ISSN Application No, 21816

Indian Journal of Automotive Technology

(Volume No. 8, Issue No. 2, May - August 2025)

Contents

ISSN Application No, 21816

A Comparative Study on Compressive Strength of Cement Mortar Cubes with Fly Ash and GGBS Produced using Different Fine Aggregates

Bugatha Adilakshmi[1], Dr. N. Victor Babu[2]

[1]P. G Student, Department of Civil Engineering Department, BABA Institute of Technology and Sciences, Visakhapatnam, AP.

[2]Head, Department of Civil Engineering Department, BABA Institute of Technology and Sciences, Visakhapatnam, AP.

ABSTRACT

River sand is the most commonly used Fine Aggregate for construction throughout India. Excessive use of river sand leads to lowering of ground water table, sand degradation and also threat to bridges, river banks and nearby structures and in the same way Cement is a major constituent material of the concrete which produced by natural raw material like lime and silica. Ordinary Portland cement is one of the main ingredients used for the production of cement mortar. But, the production of each tonne of cement involves emission of large amounts of carbon-dioxide gas into the atmosphere, a major contributor for greenhouse effect and global warming. To overcome the above backdrops, we have to go for alternatives for satisfying the requirements. The Research focused on comparing the compressive strength of cement mortar cubes produced using fine aggregates from different sources. This project involves, preparation of cement mortar cubes of CM(1:2) proportionand also cement is replaced with 25% of Fly ash and 50% of GGBS for different grades of cement (33,43 and 53) at Constant water cement ratio and tested to determine the compressive strength of cement mortar cubes for 7, 14, 28 and 54 days under normal curing conditions. Finally, preparation of graphs from obtained results for comparative analysis.

.

Keywords: Fine aggregates; River sand; Ennore sand; Stone dust; Quartz dust; Compressivestr-ength; Cement mortar

I. INTRODUCTION

River sand is most commonly used fine aggregate for construction throughout India has become highly expensive and also scarce. Natural sand is excavated from river bed impacts on environment in many ways. Due to digging of the sand from river bed reduces the water head, so less percolation of rain water in ground, which result in lower ground water level. There is erosion of nearby land due to excess sand lifting as well as it destroys the flora Fauna in surrounding areas. Since it is utmost important ingredient for cement mortar and its immersive use in construction leads to rise in economy and the requirement of material in non-availability area is also costly process. To overcome the above backdrops, we have to go for alternatives for satisfying the requirements. The most commonly used fine aggregates are river sand, Ennore sand, stone dust, quartz dust etc.,

Concrete is the most widely used construction material in civil engineering industry because of its high strength and stability. Cement is a major constituent material of the concrete which produced by natural raw material like lime and silica. Ordinary Portland cement is one of the main ingredients used for the production of cement mortar. But, the production of each tonne of cement involves emission of large amounts of carbon- dioxide gas into the atmosphere, a major contributor for greenhouse effect and global warming. This situation leads to think all people working in construction industry to do research work on cement replacing material and use of it. The construction industry is constantly looking for supplementary cementations material with the objective of reducing the solid waste disposal problem. Ground granulated blast furnace slag (GGBS) and Fly ash (FA) are the solid wastes generated by industry. To overcome from this crisis, partial replacement of cement with GGBS and fly ash can be an economic alternative.

II. OBSERVATIONS AND RESULTS

Compressive Strength Test Results

The test performed on the cubes of size 70.6mm X 70.6 mm X 70.6 mm in the compressive strength testing machine for the 3, 7, 28 and 54 days gives the compressive strength. Compressive Strength = Failure load (KN)/ Area of the cube(mm2)

A. Physical properties of different grades of cement

i. Physical Properties of Ordinary Portland cement (33 grade)

S.No	Characteristics	Values		
		cement	Cement+ 25 % flyash	Cement + 50%GGBS
1	Fineness of cement %	7	5.2	3
2	Standard Consistency, percent	29	29.5	31
3	Specific gravity	3.12	3.3	4

Table 1 Physical properties of OPC (33 grade)

ii. Physical Properties of Ordinary Portland cement (43 grade)

S.No	Characteristics	Values		
		cement	Cement+ 25 % fly ash	Cement + 50% GGBS
1	Fineness of cement %	5	4	3
2	Specific Gravity	3.17	3.4	4.11
3	Standard Consistency, percent	29.8	30	31

Table 2 Physical properties of OPC (43 grade)

iii. Physical Properties of Ordinary Portland cement (53 grade)

S.No	Characteristics			Values	
			cement	Cement+ 25 % fly ash	Cement + 50% GGBS
1	Fineness of cement %		5	3.8	2.7
2	Specific Gravity		3.18	3.42	4.13
3	Standard	Consistency,	30	30.5	31.2
	percent				

Table 3 Physical properties of OPC (53 grade)

B. Physical properties of different types of sands

I. Physical properties of Ennore sand

S.No	Physical Properties	values
1	Specific gravity	2.64
	Absorption in 24	
2	hours	0.90%

Table 4 Physical properties of Ennore sand

ii. Physical properties of river sand

S.No	Physical Properties	values
1	Specific gravity	2.65
	Absorption in 24	
2	hours	1.15%

Table 5 Physical properties of river sand

iii. Physical properties of stone dust

S.No	Physical Properties	values
2	Specific gravity	2.52
	Absorption in 24	
3	hours	1.60%

Table 6 Physical properties of stone dust

iv. Physical properties of quartz dust

S.No	Physical Properties	values
1	Specific gravity	2.75
	Absorption in 24	
2	hours	0.80%

Table 7 Physical properties of Ennore sand

C. Compressive strength values for different types of fine aggregates

ii. Compressive strength values for Ennore sand:

Type of Sand	Days	33 grade	43 grade	53 grade	33 grade 25% Flyash	43 grade 25% Flyash	53 grade 25% Flyash	33 grade + 50% GGBS	43 grade + 50% GGBS	53 grade + 50% GGBS
Ennore Sand	7	25.67	32.32	37.3	21.02	31.25	36.98	24.72	32.16	36.41
	14	30.62	39.2	45.74	27.15	31.83	37.28	28.55	38.25	44.98
	28	36.3	45.39	53.76	30.25	35.75	40.54	34.37	44.49	52.11
	56	38.12	48.28	54.97	31.25	40.07	47.64	39.09	48.9	56.47

Table 8 Compressive strength values for Ennore sand

ii. Compressive strength values for river sand:

Type of Sand	Days	33 grade	43 grade	53 grade	33 grade + 25% Flyash	43 grade + 25% Flyash	53 grade + 25% Flyash	33 grade + 50% GGBS	43 grade + 50% GGBS	53 grade + 50% GGBS
River Sand	7	23.71	28.74	34.92	18.15	27.51	33.17	22.12	27.95	34.23
	14	32.54	39.18	42.18	22.28	35.75	35.82	29.27	35.14	41.28
	28	36.74	43.57	53.19	23.15	34.14	40.28	31.98	38.15	48.27
	56	37.63	44.85	54.89	25.18	37.33	42.2	33.09	43.17	53.11

Table 9 Compressive strength values for river sand

iii. Compressive strength values for stone dust:

Type of Sand	Days	33 grade	43 grade	53 grade	33 grade + 25% Flyash	43 grade + 25% Flyash	53 grade + 25% Flyash	33 grade + 50% GGBS	43 grade + 50% GGBS	53 grade + 50% GGBS
Stone dust	7	22.16	26.03	32.75	17.15	25.87	31.86	23.75	29.75	33.98
	14	26.61	33.04	38.67	21.64	27.79	34.16	27.25	34.18	40.18
	28	29.99	40.01	44.98	22.79	31.26	36.75	31.01	40.11	47.58
	56	32.16	41.71	48.78	27.44	33.76	39.41	32.57	42.19	50.89

Table 10 Compressive strength values for stone dust

iv. Compressive strength values for quartz dust:

Type of Sand	Days	33 grade	43 grade	53 grade	33 grade + 25% Flyash	43 grade + 25% Flyash	53 grade + 25% Flyash	33 grade + 50% GGBS	43 grade + 50% GGBS	53 grade + 50% GGBS
Quartz Sand	7	27.79	35.22	39.94	21.48	28.55	32.25	26.47	33.14	37.91
	14	31.57	41.13	49.07	24.66	31.28	34.88	29.81	38.25	46.73
	28	37.94	48.12	56.33	29.02	35.15	36.25	36.14	45.37	53.41
	56	39.11	49.98	56.56	33.24	43.25	51.25	41.48	52.51	59.48

Table 11 Compressive strength values for stone dust

IV. Graphs and Discussions

i. Compressive strength Vs Different grades of cement

Compressive strength of cement mortar with different grades of cement and different types of sands at 56 days

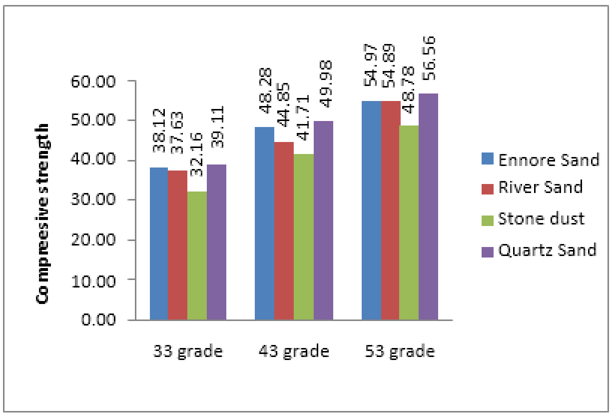

Graph 1 Compressive strength Vs Different grades of cement

Discussions:

i. From graph 1, it is observed that the cement mortar with 53 grade cement has more compressive strength compared to the cement mortar cubes produced with 33 and 43 grade cement.

ii. It is also observed that the cement mortar with quartz sand has highest compressive strength compared to cement mortar with Ennore sand, river sand and stone dust by 2.53%, 3.78% and 17.77% for 33 grade cement respectively.

iii. It is observed that the cement mortar with quartz sand has highest compressive strength compared to cement mortar with Ennore sand, river sand and stone dust by 3.40%, 10.26% and 16.54% for 43 grade cement respectively.

iv. It is observed that the cement mortar with quartz sand has highest compressive strength compared to cement mortar with Ennore sand, river sand and stone dust by 2.81%, 2.95% and13.755% for 53 grade cement respectively.

ii. Compressive strength VsNo. of days

Compressive strength of cement mortar with 33 grade cement for different fine aggregates.

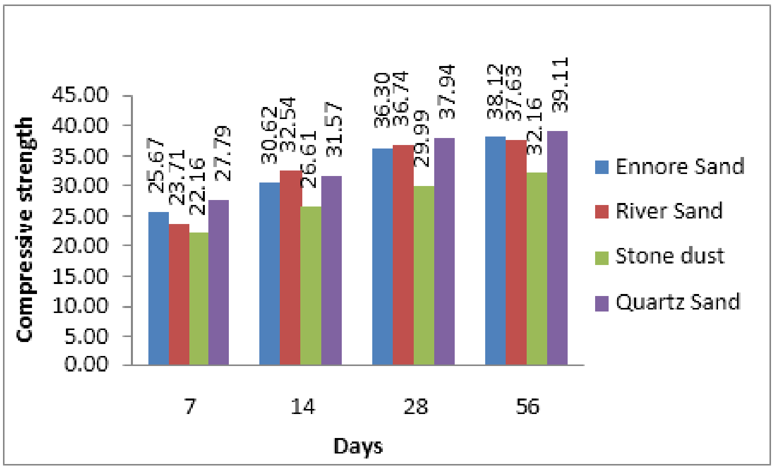

Graph 2 Compressive strength VsNo.of days

Discussions:

i. From graph 2, it is also observed that the cement mortar containing river sand has high strength for 14 days but for 56 days there is decrease in strength compared to Ennore sand and quartz sand by 1.30% and 3.93% respectively. This means that the cement mortar with river sand gains early strength compared to all other fine aggregates.

ii. It is also observed that the cement mortar with Ennore sand and river sand has almost same compressive strength at 28 days.

iii. Compressive strength VsNo. of days (fly ash)

Compressive strength of cement mortar with 33 grade cement contains 25% fly ash for different fine aggregates.

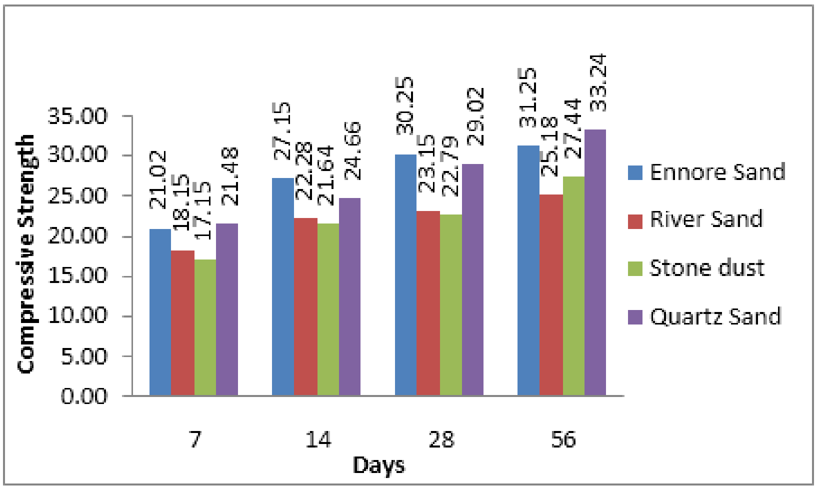

Graph 3Compressive strength Vs No.of days (fly ash)

Discussions:

i. From graph 2, it is observed that the cement mortar containing stone dust has less strength compared to cement mortar containing Ennore sand, river sand and quartz sand but from graph 3, it is observed cement mortar containing stone dust has high strength compared to river sand at 56 days when cement is replaced with 25% of fly ash.

ii. From graph 2, it is also observed that the cement mortar containing Ennore sand and river sand has almost same compressive strength but from graph 3, there is a large variation in compressive strength for cement mortar containing Ennore sand and river sand when cement is replaced with 25% fly ash.

ii. Compressive strength VsNo. of days (GGBS)

Compressive strength of cement mortar with 33 grade cement contains 50% GGBS for different fine aggregates.

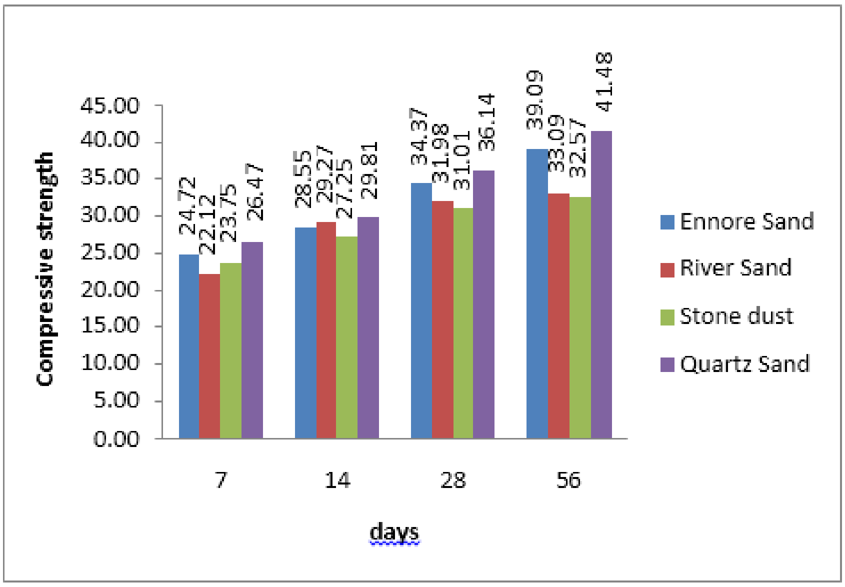

Graph 4Compressive strength Vs No.of days (GGBS)

Discussions:

i. From graph4, it is observed that the cement mortar containing stone dust has greater strength compared to river sand at 7 days but decreases from 14 days onwards.

ii. It is also observed that the cement mortar with river sand and stone dust has almost have same compressive strength at 28 and 56 days when cement is replaced with 50% GGBS.

v. Compressive strength VsNo. of days for different FA

Compressive strength of cement mortar with 33 grade cement contains 25% fly ash and 50% GGBS for Ennore sand, river sand, stone dust and quartz dust.

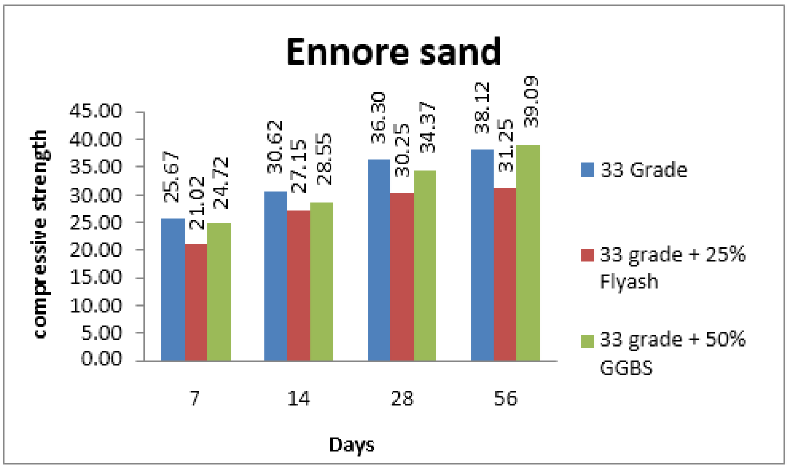

Graph 5Compressive strength Vs No.of days Ennore sand

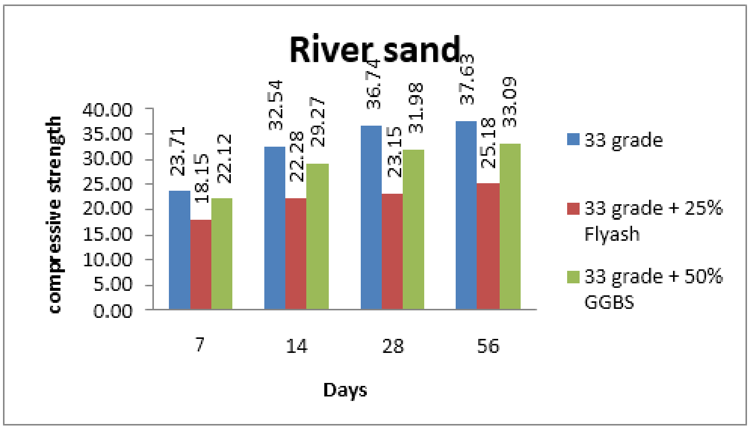

Graph 6 Compressive strength Vs No.of days for river sand

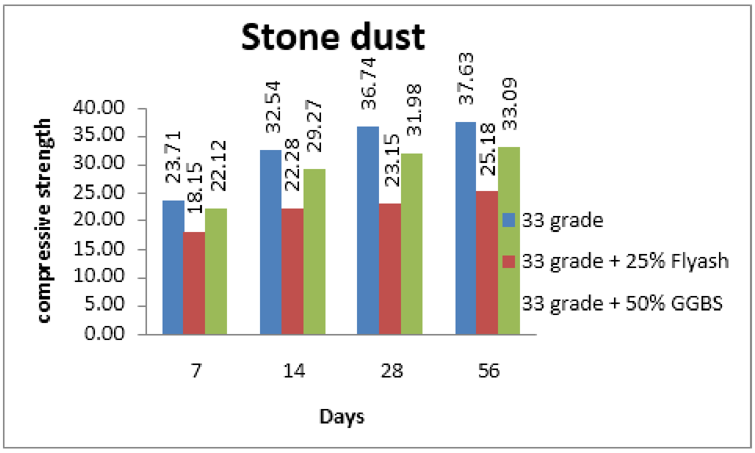

Graph 7Compressive strength Vs No.of days for stone sand

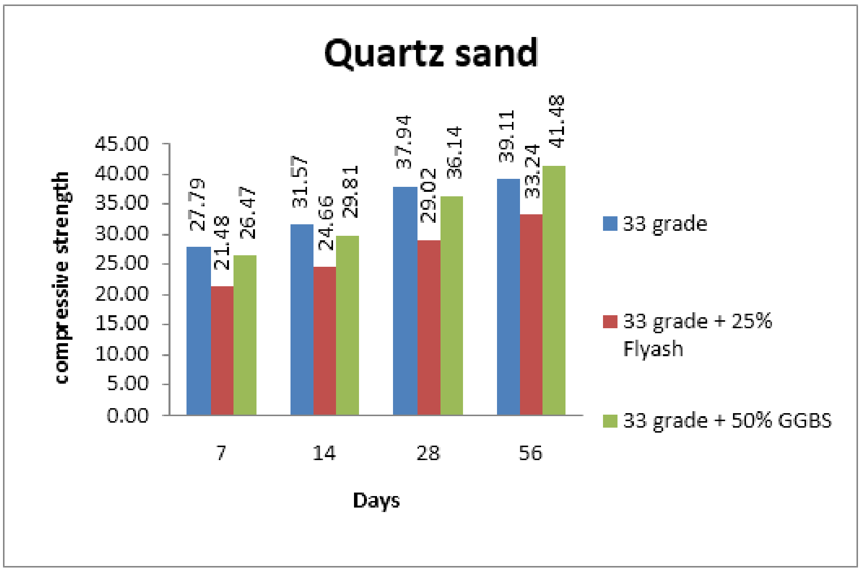

Graph 8 Compressive strength VsNo.of days for quartz sand

Discussions:

i. From graph 5 and graph 8, it is observed that the cement mortar cube containing Ennore sand and quartz sand has more strength when cement is replaced with 50% GGBS but has low strength when cement is replaced with 25% fly ash.

ii. In the same way it is observed that the cement mortar cubes containing Ennore sand and quartz sand has more strength up to 28 days but it decreases at 56 days. This means there is a gradual increase in strength when cement is replaced with 50% GGBS.

iii. From graph 6 and graph 7, it shows that the cement mortar cube containing river sand and stone dust has less strength when the cement is replaced with fly ash and GGBS.

vi. Compressive strength VsNo.of days (fly ash & GGBS)

Compressive strength of cement mortar with 33 grade cement contains 25% fly ash and 50% GGBS for different types of sands.

Discussions:

a. From graph 9, it is observed that the cement mortar cube produced with quartz sand has high compressive strength, cement mortar with stone dust has low compressive strength and the cement mortar with Ennore sand and river sand has almost have same strength for 33 grade cement at 56 days.

b. It is also observed that the cement mortar with Ennore sand and quartz sand has more strength compared with the cement mortar with river sand and stone dust when cement is replaced with 25% of fly ash and 50% of GGBS.

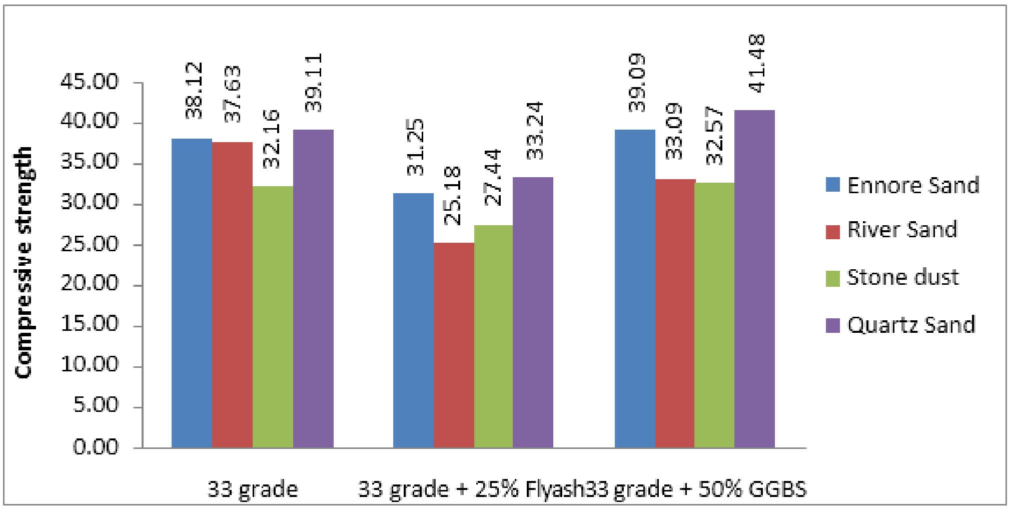

Graph 9 Compressive strength Vs No.of days (fly ash & GGBS)

V. CONCLUSIONS

The following specific conclusions can be arrived based on the study conducted on cement mortar

a. The cement mortar contains 53 grade cement has more compressive strength compared to the cement mortar with 33 and 43 grade cement.

b. It is also observed that the cement mortar with quartz sand has highest compressive strength compared to cement mortar with Ennore sand, river sand and stone dust by 2.53%, 3.78% and 17.77% for 33 grade cement respectively.

c. It is observed that the cement mortar with quartz sand has highest compressive strength compared to cement mortar with Ennore sand, river sand and stone dust by 3.40%, 10.26% and 16.54% for 43 grade cement respectively.

d. It is observed that the cement mortar with quartz sand has highest compressive strength compared to cement mortar with Ennore sand, river sand and stone dust by 2.81%, 2.95% and13.755% for 53 grade cement respectively.

e. The cement mortar containing Ennore sand and quartz sand has more strength when cement is replaced with 50% GGBS but has low strength when cement is replaced with 25% fly ash.

f. The cement mortar containing river sand has high strength for 14 days but for 56 days there is decrease in strength compared to Ennore sand and quartz sand by 1.30% and 3.93% respectively. The cement mortar with river sand gains high strength in early days compared to Ennore sand, stone dust and quartz dust.

g. The cement mortar containing stone dust has least strength compared to cement mortar containing Ennore sand, river sand and quartz sand but it is increased at 56 days when cement is replaced with 25% of fly ash.

h. If 100% cement is used, then cement mortar containing Ennore sand and river sand has almost have same compressive strength But there is a large variation in compressive strength of cement mortar containing Ennore sand and river sand when cement is replaced with 25% fly ash and 50% GGBS.

I. The cement mortar with river sand and stone dust has almost have same compressive strength when cement is replaced with 50% GGBS.

VI. REFERENCES:

1. *Abhishek Jain and Nazrul Islam "Use of flyash as partial replacement of sand in cement mortar" International Journal of Innovative Research in Science, Engineering and Technology, ISSN: 2319-8753, Vol. 2, Issue 5, May 2013.*
2. *Baali L., Naceri A., and Mehamed R., (2007), Mechanical response of mortar made with natural and artificial fine aggregates, Asian Journal of Civil Engineering (Building and Housing), 9, pp 85-92.*
3. *Baboorai, Sanjay kumar, Kumar satish "Effect of Fly Ash on Mortar Mixes with Quarry Dust as Fine Aggregate" Advances in Materials Science and Engineering, Volume 2014 (2014), Article ID 626425*
4. *B.Damodhara Reddy and I.V.Ramana Reddy, S. ArunaJyothy " Evaluation Of Mechanical And Durability Properties Of Portlandslag Cement With Partial Replacement Of Cement By Differentmineral And Chemical Admixtures" Internationalacademy of science, engineering and technology, ISSN 2278- 9987Vol. 2, Issue 1, Feb 2013, 29-38.*
5. *Chandra PrakashBastani&R. Kansal "Effect of Fine AggregateParticlesonCompressive Strength of Cement Mortar" International journal of engineering studies and technical approach ISSN 2395-0900, Volume: 1, No: 7, July 2015*
6. *C.Marthong and T.P.Agrawal "Effect of Fly Ash Additive on Concrete Properties"International Journal of Engineering Research and Applications, ISSN: 2248-9622, Vol. 2, Issue4, July-August 2012, pp.1986- 1991.*
7. *C.M.Ravikumar, M.B.Sreenivasa, K.AbdulRaheem, M.H.Prashanth, M.VijaySekhar Reddy "Experimental Studies on Strength and Durability of Mortars Containing Pozzolonic Materials" International Journal of Advanced Structures and Geotechnical Engineering, ISSN 2319-5347, Vol. 02, No. 02, April 2013.*
8. *K. ShyamPrakashand&Ch. HanumanthaRao "Study on Compressive Strength of Quarry Dust as Fine Aggregate in Concrete" Advances in Civil Engineering Volume2016 (2016), Article ID 1742769.*
9. *K. Uma Shankar & K. Suganya "Durability study of structural elements using fly ash aggregates" International Journal of Management, Information Technology andEngineering Vol. 2, Issue 1, Jan 2014, 1-6.*
10. *M. Bederina, Z. Makhloufi, A. Bounoua, T. Bouziani, M. Queneudec, "Effect of partial and total replacement of siliceous river sand with limestone crushed sand on the durability of mortars exposed to chemical solutions", Journal of Construction and Building Materials, Vol. 47, 2013,146–158*
11. *M.Haque,S. Ray, H. M. A. Mahzuz(2012) "Use of Stone Powder with Sand in Concrete and Mortar: A Waste Utilization Approach", ARPN Journal of Science andTechnology, vol. 2, No. 7*
12. *M.R.Karim,M.F.M.Zain,M.Jamil,F.C.Lai,M.N.Islam.(2011) "Strength development of mortar and concrete containing fly ash:A Review". International Journal of thePhysical Sciences Vol. 6(17), pp. 4137-4153.*
13. *M.N.N.Khan, M.Jamil, A.B.M.A.Kaish, M.F.M.Zain, M.R.Karim "An Experimental Study on the Strength of Mortar due to Filler Effect of PozzolanicMaterials"International Journal of Advanced Structures and Geotechnical Engineering, ISSN 2319-5347, Vol. 03, No. 02, April 2014.*
14. *O. A. Cabrera , L. P. Traversa , N. F. Ortega ,"Effect of crushed sand on mortar and concrete rheology", Materiales de Construccion, 61(303), 401-416, (2011)*
15. *Praveen Kumar and Radhakrishna "Strength and workability of cement mortar with Manufactured sand" International Journal of Research in Engineering and Technology eISSN: 2319-1163 | pISSN: 2321-7308*
16. *Priyanka A. Jadhav, Dilip K. Kulkarni "Effect of replacement of natural sand by manufactured sand on the properties of cement mortar", International Journal of Civil and Structural Engineering, ISSN 0976 – 4399, Volume 3, No 3, 2013*
17. *Shaswata Mukherjee, SarojMandal, Adhikari.U.B "Study on the physical and mechanical property of ordinary portland cement and fly ash paste" InternationalJournal Of Civil And Structural Engineering, ISSN 0976 –4399, Volume 2, No3, 2012*
18. *S. P. S. Rajput, M. S. Chauhan, "Suitability of Crushed Stone Dust as Fine Aggregate in Mortars" International Journal of Emerging Technology and Advanced Engineering ISSN 2250-2459, ISO 9001:2008 Certified Journal, Volume 4, Issue 3, March 2014*
19. *Sunil N Manjunath and P V Sivapullaiah, M Prasanna Kumar "Implication of partial replacement of cement with FA and sand by GBS on setting time and workability ofMortar" International Journal of Research in Engineering and Technology, eISSN:2319-1163 | pISSN: 2321-7308*
20. *Tasniahoque& Muhammad harunur Rashid "Influence of Stone Dust as Partially Replacing Material of Cement and Sand on some Mechanical Properties of Mortar" International Journal of Advanced Structures and Geotechnical Engineering ISSN 2319-5347, Vol. 02, No. 02, April 2013.*
21. *Vinit Kumar Singh, VikasSrivastava, V.C Agarwa, Alvin Harison "Effect of Fly Ash as Partia Replacement of Cement in PPC concrete" International Journal ofInnovative Research in Science, Engineering and Technology, ISSN(Online): 2319-8753, ISSN (Print) : 2347-6710 (An ISO 3297: 2007 CertifiedOrganization), Vol. 4, Issue 7, July 2015.*

Dynamic Analysis on R31 Steam Turbine Blade

Pothina Surya Rao *, Sidagam Ananth**

* Assistant. Professor, Mechanical department, BITS Vizag, Visakhapatnam, India.

** Assistant. Professor, Mechanical department, BITS Vizag, Visakhapatnam, India.

*** M.Tech graduate, Mechanical department, BITS Vizag, Visakhapatnam, India.

A B S T R A C T

The Steam turbine blades are subjected to in-plane load because of fluid or aerodynamic pressures so the blades are subjected to high dynamic loadings. It is necessary to do vibration analysis to know the dynamic characteristics of the material as they are working at high speeds. The X20cr13 steel material R31 turbine blades are used in 7.5MW BBC as turbine rotor in power plants. Flow of the super heated steam in steam turbines causes failure of blades due to high temperature working condition, high rotational speeds and corrosion of blade due to the purity of steam.

The existing X20 turbine blade is replaced with the composite material without the increase in the stresses. Two types of composites are taken with a matrix and reinforcements. One is glass-ceramic matrix systems reinforced with silicon carbide and silicon carbide reinforced with the aluminum matrix. Aluminum silicon carbide compare the mode of vibrations for the existing and newly design composite plates by using CATIA V5 R21 and ANSYS 15.0 software's.

Secondly, the existing blade made of X20Cr13 is replaced with the metal matrix composite aluminum silicon carbide. Metal matrix Composites possesses high-temperature capability, high thermal conductivity, low CTE, and high specific stiffness and strength. Addition of SiC into the aluminium matrix produces a resulting composite with the low density of aluminium but a higher modulus similar to steel. When the existing X20 material turbine blade is replaced with the composite material AlSiC MMC and Pyrosic, the von mises stresses are very much reduced. The life of the blade is also increased by using composite materials.

Keywords: ANSYS; CATIA V5; Stress Analysis; Composite; Fatigue; Modal Analysis.

1. INTRODUCTION

A steam turbine is a device that extracts thermal energy from pressurized steam and uses it to do mechanical work on a rotating output shaft. Steam turbines are made in a variety of sizes ranging from small 0.75 kW units used as mechanical drives for pumps, compressors and other shaft driven equipment, to 15,00,000 kW turbines used to generate electricity. There are several classifications for modern steam turbines.

The steam turbine is a form of heat engine that derives much of its improvement in thermodynamic efficiency from the use of multiple stages in the expansion of the steam, which results in a closer approach to the ideal reversible expansion process. The main of parts of turbine are rotating shaft, turbine blades, nozzles, gears and driven mechanism. In this turbine blade is one of the fundamental element of steam turbine where the steam flows is hits the turbine.

Turbo machinery blades are classified into two categories depending on their manner of operation as either impulse or reaction blades. The failures of these blades in practical working conditions cause several damage and loss. So this leads to study of turbine blades for better performances of steam turbines. The break down and failures of turbine machineries have been influencing such as consequential damages, hazards to public life and most importantly the cost repairs.

To avoid these, it is obvious that the blade of turbo machinery must be made structurally stronger, that means not in dimensions and/or use of materials of construction, but keeping the operating stresses well within the limits. The blade fatigue failure is one of the major sources of outages in any steam turbines and gas turbines which are due to high dynamic stresses caused by blade vibration and resonance within the operating range of machinery.

To protect blades from these high dynamic stresses, friction dampers are used. To survive in this difficult environment, turbine blades often use exotic materials like super alloys and many different methods of cooling, such as internal air channels, boundary layer cooling, and thermal barrier coatings.

2. LITERATURE REVIEW

One of the important thing is material selection with respective operating conditions and quality of steam. The vast use of turbo machinery blades lead to significant amount of research over the years. Due to its wide range of application in the practical field, it is important to understand the nature of deformation, vibration and stability behavior of X20 turbine blades.

Philip Dowson and derrick Bauer [1] stated a thesis on turbine blade “Selection of materials and material related process for steam turbiSpediel [2] highlighted the satisfactory corrosion fatigue resistance of x20CrMoV121 steel in a good purity steam. However, the growth of fatigue cracks in 12 percent chromium steels in greatly enhanced by the chloride solutions at low cyclic stress intensities and high mean loads. Spediel also illustrated how the deltakth greatly reduced by the presence of the certain environments.

Forces on Large Steam Turbine Blades is investigates RWE Npower Mechanical and Electrical Engineering power industry [3] in Germanynes in these oil and petrochemical industry”. Steam Turbine rotors are designed with a significant factor of safety, the operating forces and stresses calculated, large steam turbine blades are manufactured from 12% chrome high alloy steels where maximum design stress values of 200-300 N/mm2 are permissible. vibration analysis of a steam turbine by R.s.Mohan, A.Sekhar and A.s. Shekar [4] stated that dynamic steam turbine blade in computational environment is carried out by the reliability of these blades very important for the successful operation of steam turbines . In order to gain physical insight into the flexural dynamics of such turbine blade with the inclusion of the rotor dynamics effect the turbine blade was approximated as symmetry air foil cross section fixed on rigid disc. Wear Characteristics in Al- SiC Particulate Composites and the Al-Si Piston Alloy Z. Hasan1, R. K. Pandey, D.K. Sehgal [6] Al-Si alloy with near eutectic composition has been conventionally used as a piston material for automobile applications. It is required to possess high abrasive wear resistance for enhanced life of the engine. The alloy is known to have fairly good wear resistance due to increased percentage of silicon present in fine form. In the present investigation, Al-SiC particulate composites have been studied for their wear resistance against emery paper (400 grit SiC particles) counter f ace and a comparison has been made with existing piston alloy i.e. Al-Si alloy. Aluminum (Al-6063)/SiC Silicon carbide reinforced particles metal-matrix composites (MMCs) are fabricated by melt-stirring technique by K.L.Meena, Dr.A.Manna [7]. The MMCs bars and circular plates are prepared with varying the reinforced particles by weight fraction ranging from 5%, 10%, 15%, and 20%. The average reinforced particles size of SiC are 220 mesh, 300 mesh, 400 mesh respectively.

3. CALCULATION OF FORCES ON BLADES

Forces acting on the blades of the rotor in general have two components namely tangential (Ft) and axial (Fa). These forces result from the steam momentum changes and from pressure differences across the blades. These steam forces are evaluated by constructing velocity triangles at inlet and outlet of the rotor blades. The rotor blades considered for analysis are untwisted and same profile is taken throughout the length of the blade. If the steam forces are assumed to be distributed evenly, then the resultant acts through the centroid of the area. At the inlet of the steam turbine rotor blades,

Absolute flow angle $\alpha 2 = 23.850$ Absolute velocity $V2 = 462.21$ m/s

The velocity triangles at inlet of Gas turbine rotor blades are constructed as shown.

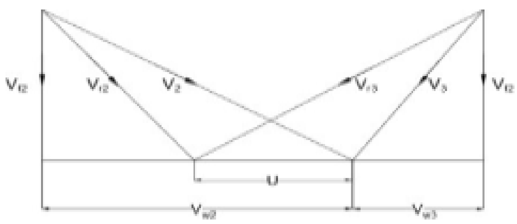

Figure 3.1 Inlet & Exit velocity triangles of steam turbine rotor blades

Diameter of blade midspan D = 1.65 m. Design speed of turbine N = 1800 r.p.m.
Peripheral speed of rotor blade at its midspan $U = \pi DN/60 = 60\pi$ m/sec-- (1)

From the velocity triangles in figure we get, Whirl velocity Vw2 = 422.74 m/s
Flow Velocity Vf2 = 198.89 m/s Relative velocity Vr2 = 265.09 m/s Blade angle at inlet $\theta 2 = 45$ 0

At the exit of Gas turbine rotor blades,
Flow velocity Vf3 = 189.42 m/s
Relative flow angle $\theta 2 = 37.88$ 0
From the velocity triangles (Figure), we get

Whirl velocity at exit Vw3 = 2.805 m/s Relative velocity at exit Vr3 = 293.83 m/s

4. MODELLING OF TURBINE BLADE

Using Catia module the profile drawing in the figure 4.1of blade is converted into 2D drawing as in the figures 4.2 and 4.3, root section of the blade and area foil section of the respectively by the various commands in the Catia module as same as measurements in the profile drawing. Commands like points, circles splines, rectangles, squares and work bench are used to generate 2D drawing. In 2d diagram is extrudes in the work bench by pad and pocket commands. The figure 4.3 Catia model of the blade shows the 3D view of the blade.

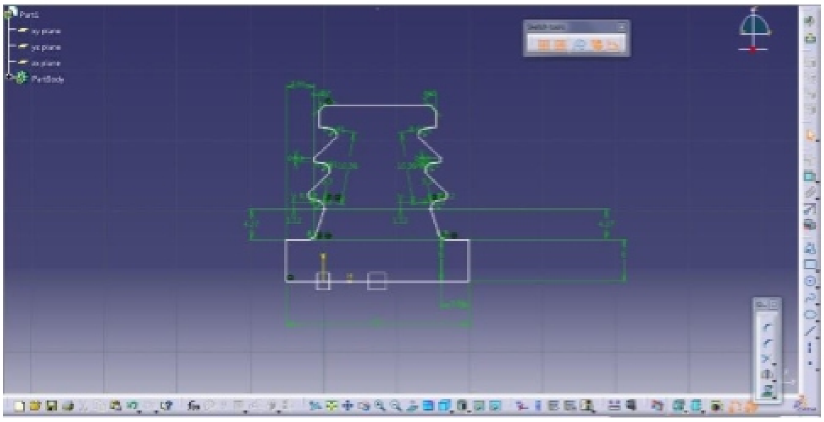

Figure 4.1 Root Section of the Blade

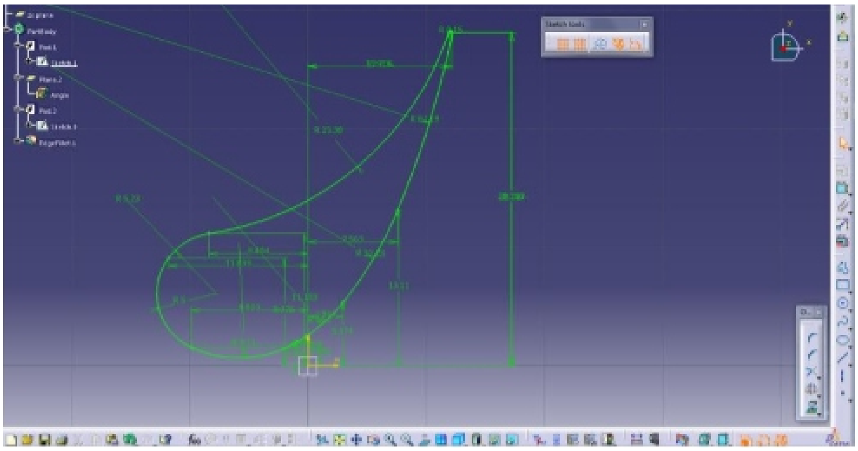

Figure 4.2 Aerofoil Section of the Blade

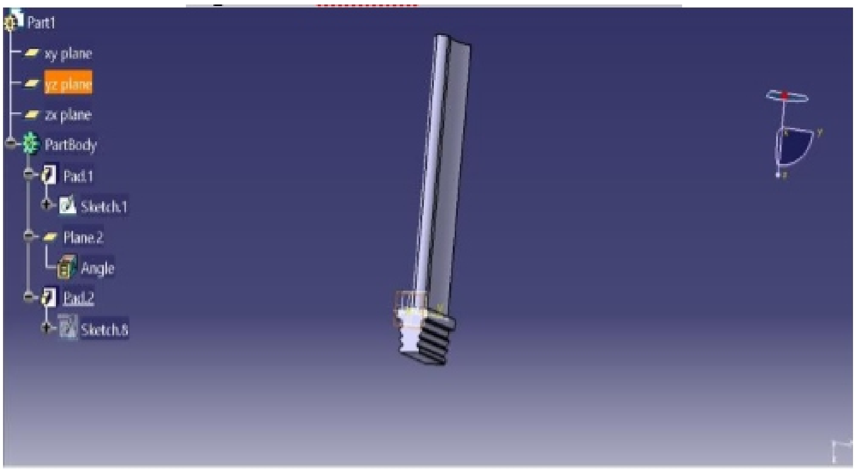

Figure 4.3 CATIA Model of the Blade

5. ANALYSIS OF TUBINE BLADE BY ANSYS

Auto mesh is done in ANSYS workbench to solve the differential equations, which are a combination of structured and unstructured mesh. The imported file geometry undergoes meshing after which boundary conditions are applied to the physical domain

Tetra Mesh is done in ansys solver as shown in below figure 5.1

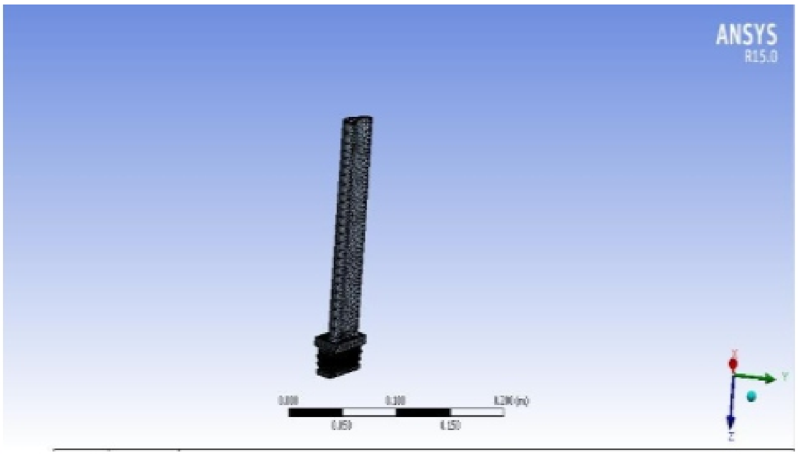

Figure 5.1 Tetra- Mesh

Tangential force Ft =310.4N
Axial force Fa = 7.473 N
Centrifugal force Fc = 7737.5 N

The above three forces are applied as boundary conditions to the turbine blade as shown in fig.5.2

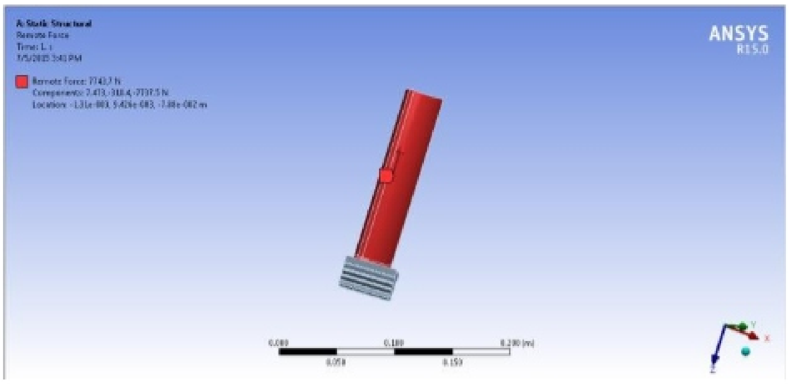

Figure 5.2 Static loading on X20 material rotor

Static structural analysis is carried for existing blade material and by followed the two new proposed composite blade material and the solution data for them is presented below.

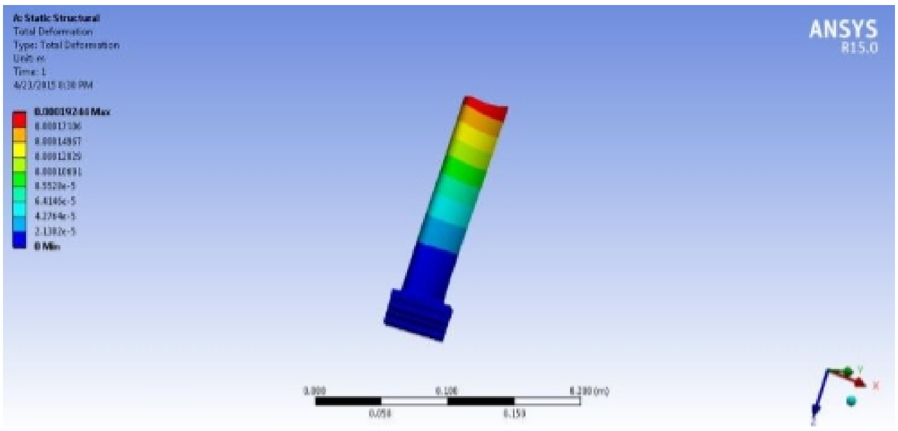

Figure 5.3 X20 Blade deformation

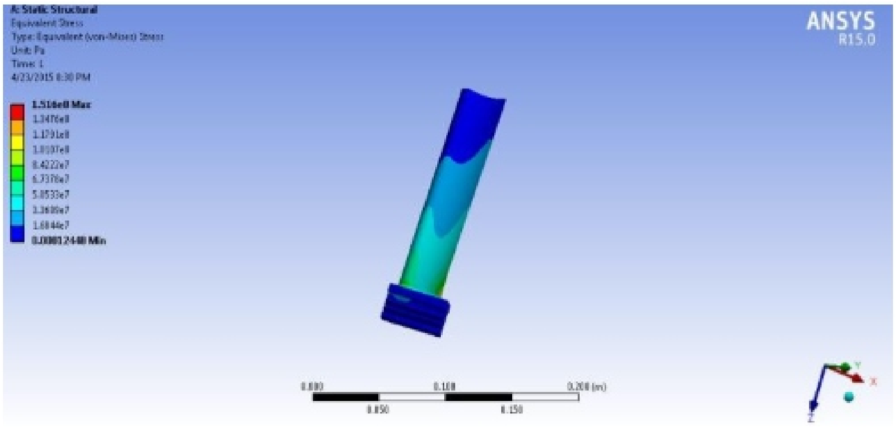

Figure 5.4 X20 Blade Von-Mises Stress

From the above figure 5.3 and 5.4 of X20 Cr13 material blade from Static analysis solution, have a deformation 0.192mm and the von mises stress is 1.516Pa for the loading condition of tangential force 310.4N, axial force 7.473 N and centrifugal force 7737.5 N.

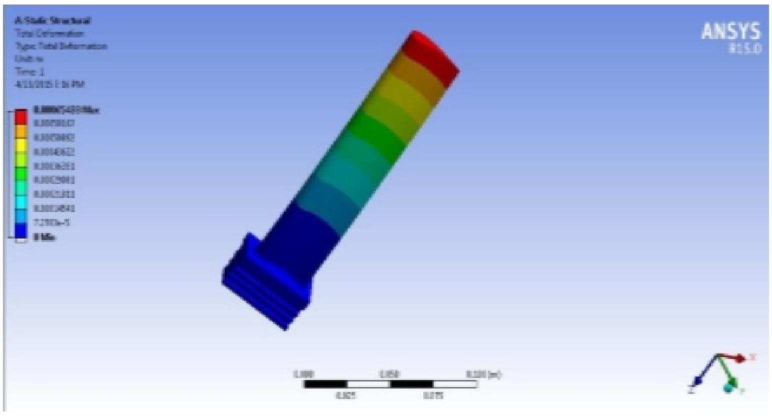

Figure 5.5 AlSiC blade deformation

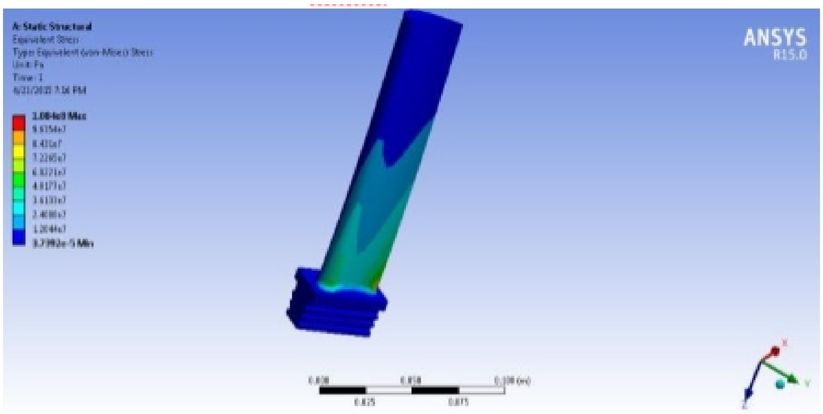

Figure 5.6 AlSiC Von-Mises Stress

From the above figure 5.5 and figure 5.6 of Al/SiC material blade from Static analysis solution have a deformation 0.65mm and the von mises stress is 1.084e8Pa for the loading condition of tangential force 310.4N, axial force 7.473 N and centrifugal force 2612.6 N.

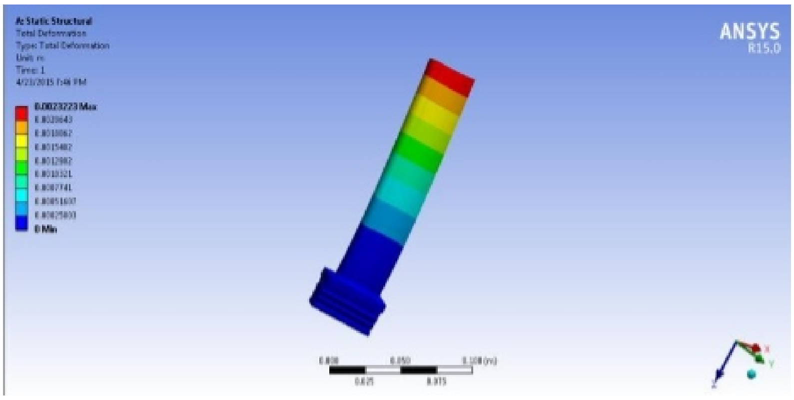

Figure 5.7 Pyrosic blade deformation

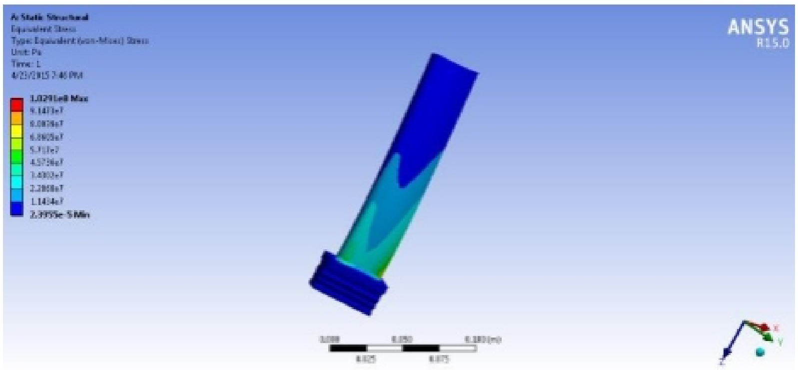

Figure 5.8 Pyrosic Von-Mises Stress

From the above figure 5.7, figure 5.8 of Pyrosic composite blade from Static analysis solution have a deformation 0.65mm and the von mises stress is 1.084e8Pa for the loading condition of tangential force 310.4N, axial force 7.473 N and centrifugal force 1848.9 N.

Fatigue analysis

In operating conditions many parts may does not fail initially, they often fail in service due to fatigue failure caused by repeated cyclic loading. In practice, loads significantly below static limits can cause failure if the load is repeated sufficient times. The main objective of fatigue analysis is to characterizing the capability of a material to survive and how many cycles can a component may experience during its lifetime. Types of Fatigue Analysis available in ansys are Strain Life, Stress Life, and Fracture Mechanics.

Stress Life is based on S-N curves (Stress – Cycle curves). This is concerned with total life and does not distinguish between initiation and propagation. In terms of cycles, Stress Life typically deals with a relatively high number of cycles. High number of cycles is usually refers to more than 10e5 cycles.

After completing the static structural analysis the solution module is transferred into Fatigue analysis module, and the boundary conditions are same as structural analysis. In setup select the fatigue analysis type as stress life. In solution insert life as a required output, and then run for solution.

After performing the fatigue analysis, the following results are presented below. Figure 5.9 figure 5.10 and figure 5.11 shows the fatigue results of the blade.

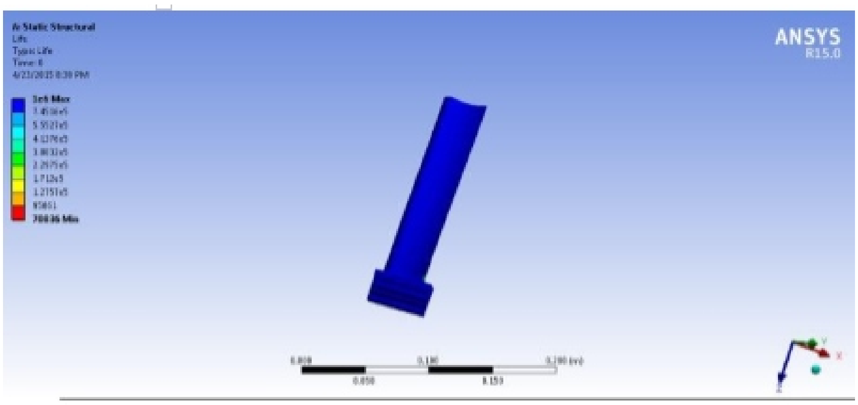

Figure 5.9 X20 Blade Fatigue Life

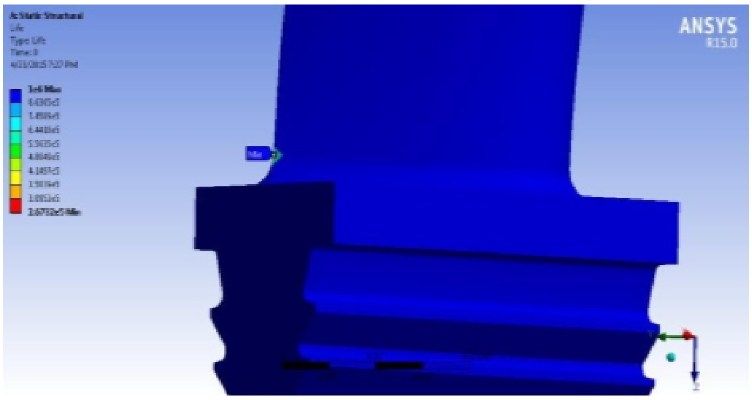

Fig 5.10 AlSiC Blade Fatigue Life

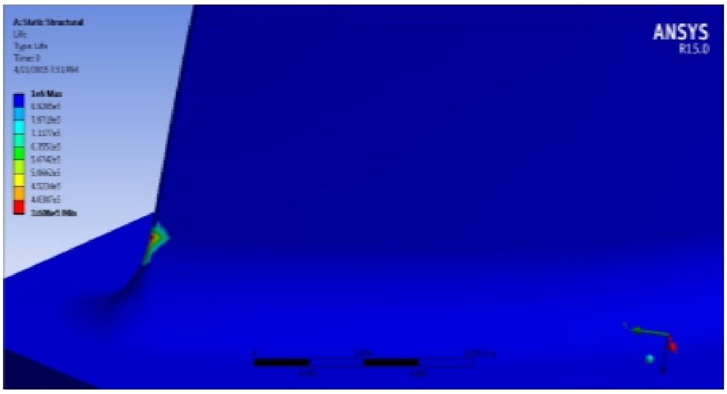

Figure 5.11 Pyrosic Blade Fatigue Life

From the above figures 5.9 5.10 and 5.11 of different material blades by fatigue analysis solution have a fatigue life as 70836 cycles for X20 cr13, 2.6732e5 cycles for AlSiC, 3.606e5 cycles Pyrosic respectively.

6. RESULTS AND DISCUSSIONS

From the solution of Static structural analysis results, we have the following data

Blade Material	Von-Mises Stress (Pa)	Deformation (m)
X20 cr13	1.52E+08	0.00019244
AlSiC	1.08E+08	0.00023223
Pyrosic	1.03E+08	0.00065433

Table 6.1 Comparison of Stress, Deformation of different Materials

The tangential and axial forces acting on the X20, Al/SiC and Pyrosic blade are same ie 310.4N and 7.473N, but the centrifugal force acting on the blades are vary ie. X20, Al/SiC and Pyrosic blades are 7737.5N, 2612.6N and 1848.9N. The Von misses stresses for X20, Al/SiC, Pyrosic are 1.516e8Pa, 1.084e8Pa, 1.029e8Pa. There is much variation in the centrifugal force acting on the blades of three materials these variation caused the reduced stresses.

The Von mises stresses induced in the blade by three materials are below the corresponding material yield stresses, so all the designs are safe in this working condition. The factor of safety for the existing X20 material is slightly high when compared to Al/SiC MMC. The factor of safety for the Pyrosic composite blade is high when compared to X20 material blade.

RESULT AND DISCUSSION ON FATIGUE ANALYSIS

This result contour plot shows the available life for the given fatigue analysis. In this the loading is of constant amplitude, this represents the number of cycles until the part will fail due to fatigue. In the given load history represents one hour of loading and the life was found to be 120, the expected model life would be 120 hours

Blade Material	Fatigue Life (cycles)
X20 cr13	70836
AlSiC	267320
Pyrosic	360600

Table 6.2 Fatigue life of different blade materials

By the results of the above table X20 material blade has low life of 70836 cycles when compared to Al/SiC 2.6e5 cycles and Pyrosic 3.6e5 cycles. The composite materials have good strength and stiffness there by fatigue life is increased in the results. The fatigue failure is occurred at the end of the aerofoil profile nearer to the root section, here increase the thickness of the aero foil may increase the blade life.

REFERENCES

[1] Philip Dowson and derrick Bauer,(2008) ‘selection of materials and material related process for steam in the oil and petro chemical industry, proceedings of the thirty-seven turbo machinery symposium.

[2] Spediel, batte and Murphy (1981), threshold intensity and fatigue strength reduction, proceedings of the thirty-three turbo machinery symposium.

[3] Forces on large steam turbine blades rne Npower mechanical and power industry Germany.

[4] R Mohan, A sekhar and a s sekhar (2001), dynamic stress of the steam turbine blade, iijret journal p 783.

[5] M. A. Occhionero, K. P. Fennessy, R. W. Adams, and G.J Sundberg, ‘AlSiC Base plates for Power IGBT Modules design, Performance and Reliability’, Ceramics Process Systems Chartley.

[6] Z. Hasan1, R. K. Pandey2*, D.K. Sehgal, ‘Wear Characteristics in Al-SiC Particulate Composites and the Al-Si Piston Alloy ‘ Vol.10, No.14 pp.1329-1335*

[7] K.L.Meena, Dr.A.Manna, Dr.S.S.Banwait, Dr.Jaswanti, “An Analysis of Mechanical Properties of the Developed Al/SiC-MMC’s” American Journal of Mechanical Engineering, 2013, Vol. 1, No. 1, 1

[8] S.Chaitanya, B.V.Ramana Murty “Mass optimization of wheel rim” International Journal of Engineering Trends and Technology (IJETT) – Volume 26 Number 3- August 2015

[9] Joseph Mills-Brownan, Kevin Pottera, SteveFosterb, Tom Bathob (2013) Thermal and tensile properties of polysialate composites.

[10] Joseph Mills-Brown Kevin Potter, Steve Foster, Tom Batho(2013) The development of a high temperature tensile testing rig for composite laminates métal matrix Composites for Space Applications by Suraj rawal in Jow journal.

[11] J s Rao, and K.Ch.Peraiah, Udai kumar singh,’estimation of the dynamic stress in the turbines blades under low volumetric flows’ p 348.

[12] SureshBabu G, Raviteja Boyanapalli, Raja Sekhara Reddy Vanukuri, Prudhvi Gogineni, Janakinandan Nookala, Goutham Kumar Yarlagadda, VinayBabu Gada Identification of Critical Speeds of Turbine Blade Along with Stress Stiffing and Spin Softening Effects International Journal of Innovative Technology and Exploring Engineering (IJITEE) ISSN: 2278- 3075, Volume-2, Issue-5, April 2013.

[13] P.Mestanek, "Low cycle fatigue analysis of a last stage steam turbine blade", Journal of applied and computational mechanics, 2008.

[14] "TARTIBU L.K, KILFOIL M and VAN DER MERWE A.J." Vibration analysis of a variable length blade wind turbine, International journal of advances in engineering & technology, 2012.

ISSN Application No, 21816

Design and Analysis of Single Point Cutting Tool by Varying Rake Angle

Ananth Sidagam[1], Gembali Vikram Kumar[2]
Asst. Professor Dept of Mechanical Engineering BITS Vizag
M. Tech graduate Dept of Mechanical Engineering BITS Vizag

A B S T R A C T

In the engineering industry Metal cutting process forms the basis and is involved indirectly or directly in the manufacture of every product of our modern civilization. The study of metal cutting is very important and knowledge in the fundamentals of machining of materials is essential. Theory of metal cutting will help to develop a scientific approach in solving problems encountered in machining.

In this project "Design and Analysis of Single Point Cutting Tool by varying rake angle", by varying rake angles the metal cutting theory is studied and this have been extended to tool-geometry, materials used and its properties, working conditions and its characteristics, effects of variable parameters like feed, cutting speed, and depth of cut during the machining process.

This project includes modeling of single point cutting tool with commercial angles in CATIAV5R20 and then the analysis is done in ANSYS15.0. After post processing the results of analysis, we modified the geometrical design and designed various tools with different back rake angles, analyzed them individually.

Keywords: cutting tool; cutting speed; feed; depth; Catia; Ansys.

1. INTRODUCTION

The study of machine tools and metal cutting is one of the most fascinating experiences. Material machining is done to adopt higher surface finish, complex geometric shapes, close tolerances.

Material removal is most expensive one when compared to all the manufacturing processes available. This is because, to achieve the desired shape some amount of material will be removed in the form of chips from the raw material and also a lot of energy should be expanded in the process of material removal. So, when there is no option for manufacturing process this type of material removal process is chosen as other alternative. However, all components undergo in the removal operation invariably at one point or the other..

Machine tool can be defined as holing components which holds the cutting tools and it have ability to remove metal from the work-piece, to obtain the desired shape with given configuration, size and finish. Machine tools are also known as mother machines because, without them components cannot be produced in desired form.

Machining is the process of removing the unwanted material from parent material of the metal by using a machine tool. This metal cutting can be done either by single point cutting tool or multi-point cutting tool. Some of the metal cutting operations are Drilling, Milling, Boring, T urning, Planning, Shaping, Broaching, etc. The machining operation is significantly affected by physical properties and chemical composition properties of the metal of the work piece, tool geometry and its material used.

There are two types of metal cutting by a single point cutting tool. They are orthogonal cutting and oblique cutting.

ORTHOGONAL CUTTING:

During this cutting process, the cutting face of the tool will be at right angle to the line of action of the tool then it is called orthogonal cutting and the direction of the chip flow will be perpendicular to the cutting edge. This type of cutting produces sharp corners. In the orthogonal cutting, the tool life will be less. Generally parting off, broaching and slotting operations are done in this method.

There are two forces orthogonal cutting. They are Cutting and Feed forces. The Radial force is zero because the face of the cutting tool is at right angle to the line of action of force.

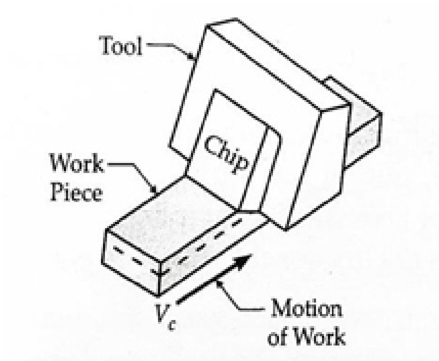

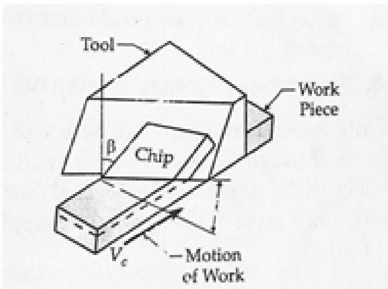

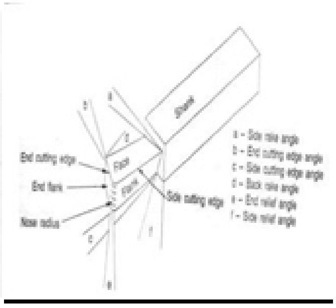

Figure 1.1: Orthogonal Cutting Figure 1.2: Oblique Cutting Figure 1.3: Geometry of a Single-point Cutting Tool

Under the process of cutting, if the cutting face of the tool is inclined and it is less than right angle to the line of action of the tool then it is known as oblique cutting. Here, the direction of the chip flow will make an angle to the cutting edge. This cutting produces chamfer at the end of cut.

In oblique cutting, the tool life will be more. Generally all machining operations are done in this method. There are three mutually perpendicular components of cutting forces at the cutting edge of the tool. The cutting edge may or may not be longer than the width of the cut. Cutting forces greater than Feed force greater than Radial force. The forces are in the order of:

$$Fc > Ft > Fr$$

The geometry of single point tool consists of three orthographic views. A single-point tool consists of the shank or the body and a neck, which is known as the operating end. The use of the shank is to hold tool in the tool post or tool holder. The tool neck has the following elements: Face, Cutting Edges, Flank, and Nose. Here face is the surface on which the chip impinges from the work piece along which it flows as it is separated from the work. The flanks are the two surfaces of the tool facing the work. They are called the main flank or the side flank and the end flank or auxiliary flank.

In the process of metal cutting edges are formed by the intersection of the flank and the face. They are called the main or side cutting and end cutting edge. The side or the main cutting edge is the main sharp edge for the cutting process. This is formed by the intersection of side flank and the face. The end cutting edge is formed by the intersection of the face and the end flank. The nose is the element formed at the junction of the end cutting edges and side cutting edge. This junction or the nose has a curve of small radius known as nose radius.

Cutting tool angles:

The geometry of the cutting tool is defined by five angles these are described below:

• **Side Rake Angle:** Side rake angle is the angle between line parallel to the base of the tool and the tool face and is measured in a plane perpendicular to the side cutting edge and the base. This angle gives the slope of the face of the tool from the cutting edge.

• **Back Rake Angle:** Back rake angle is also commonly called rake angle. It is the angle between the normal to the machined surface at the cutting edge to the face of the cutting tool. Rake angles may be positive, negative or zero. The strength of the tool is a function of rake angle. A tool with a positive rake angle will have less cross-sectional area for resisting the cutting forces. Hence, the strength of the tool is maximum when rake angle is negative.

• **Relief Angle:** The relief angle is the angle between the tangent to the machined surface at the cutting edge and the flank of the cutting tool. The side face of the flank forms side angle and the end face of the flank form relief angles. The relief angles enable the flank of the cutting tool to clear the work-piece surface and prevent rubbing. These relief angles are also referred to as clearance angles.

• **End Cutting Edge Angle:** This is the angle formed by the end cutting edge with the machined surface is called end cutting edge angle. This angle provides a clearance for that portion of that cutting edge, which is behind the nose radius. This angle reduces the length of the cutting edge in contact with the work. It is undesirable to have a cutting edge, just contact the work surface without actually cutting. This results in rubbing action, causing more tool wear and may spoil the surface finish.

• **Side Cutting Edge Angle:** Angle formed by the side cutting edge with the normal to machined surface is known as side cutting edge angle. It is essential for enabling the cutting tool at the start of the cut to the first contact the work back from the tool tip. A large side cutting edge angle increases the force component, which tends to force the cutting tool away from the work-piece.

2. CUTTING TOOL MATERIALS

Cutting tool performance will always depend on the material used. This material used in maching application should have properties such as hot hardness, wear resistance, and toughness. Here, toughness and wear resistance are two characteristics, which are, independent and the gain of one results in the loss of another.

By considering the needs of the industry, e.g. good surface finish, higher rates of production, close tolerances, etc., various tool materials have been developed. The development of new tool materials came into existence in many cases has brought the necessary for a change in the design trend of machine tools and to use the potentialities of tool materials for higher productivity. The tool materials developed include high. speed steels, tool steels, Ceramics, Synthetic diamond and Carbides.

High Speed Steel

Alloying steel with Tungsten, Chromium, Molybdenum, etc. produces alloy steel known as high speed steel (HSS). It can retain the hardness up to 600 0C. Owing to its superior hot hardness and wear resistance, it can be widely used. It can operate at cutting speeds 2-3 times greater than carbon steels. HSS can be classified into three types based on alloying elements and their percentage:

• **8-4-1 HSS:** In this alloy steel, it contains of 1% Vanadium, 4% Chromium, and 8% Molybdenum and it functions as effectively as 18-4-1 HSS. It has excellent toughness and cutting ability. This type of steel is also known as Molybdenum based HSS.

• **18-4-1 HSS:**In this alloy steel, it contains1% Vanadium, 4% Chromium, and18% Tungsten. This type of steel has good stability and provides good hot hardness. This type of steel is known as Tungsten based HSS.

• **Cobalt based HSS:** This steel contains of 2-15% Cobalt. It increases wear resistant and the hot hardness. As the hot hardness is very high it can be operated at very high speeds. This steel is also known as super high speed steel.

Carbides

In carbide mostly we will find tungsten carbide as its primary ingredient. In the purpose of steel machining carbide will be much suitable and it consists of 8% Cobalt, 10% Titanium and 82% Tungsten carbide. These carbides have very high hardness, temperatures and have high thermal conductivity. These carbides have a strong tendency in forming of pressure welds at low cutting speeds and hence they should be operated at high speeds compared to those used for HSS tools.

Turning

In this operation excess material is removed from the work piece to produce cylindrical surface or a cone shaped surface. This operation is carried out on lathe. Various types of turnings on lathe can be performed are taper turning, eccentric turning and straight turning.

Forces in Turning:

The forces in a turning operation are very important in the design of machine tools. While machining the tool must have ability to withstand all the forces without causing much significance to vibrations, deflection or chatter during the time of operation.

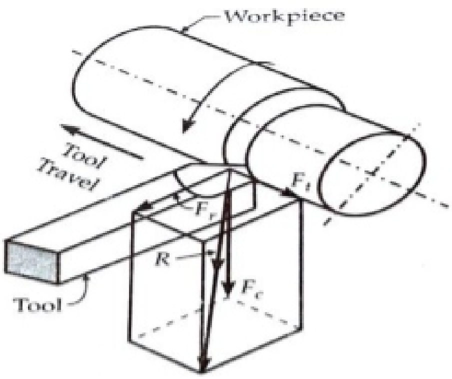

Figure 1.4: Forces acting on a Single Point Turning Tool

There are three principal forces during a turning process:

• **Cutting or Tangential Force:** Cutting force acts directly on to the work piece and the tool tip acts downward allowing deflection of the work-piece upward. Cutting forces gives force on the tool for the required cutting operation. Cutting force depends on the material.

• **Feed or Thrust Force:** Feed force acts in longitudinal direction and pushes the tool away from chuck. So it is also called as thrust force.

• **Radial Force:** Here the force acts in the radial direction and it tries to push the tool away from work-piece.

In case of turning operation, cutting force, radial force and tangential force (Fc, Ft and Fr) can be easily determined using the relation for resultant R:

$$R = \sqrt{(F_c^2 + F_t^2 + F_r^2)}$$

modelling of tool in catia

Geometry of the Tool

The geometry of the tool that used to develop part modeling in CATIA V5R20 is given below

Width (B) - 25

Height (H) – 40

H/B ratio = 1.6

Back Rake Angle (degrees)	Side Rake Angle (degree s)	End Relief Angle (degrees)	Side Relief Angle) (degrees)	End Cutting Edge Angle (degrees)	Side Cutting Edge Angle (degree s)	Tool Radius (mm
70	100	50	50	150	150	0.5
80	100	50	50	150	150	0.5
90	100	50	50	150	150	0.5
100	100	50	50	150	150	0.5

Table 3.1: Geometry of the Tool

Modelling of tool

The rough sketch of the tool shank in CATIA tool is shown below

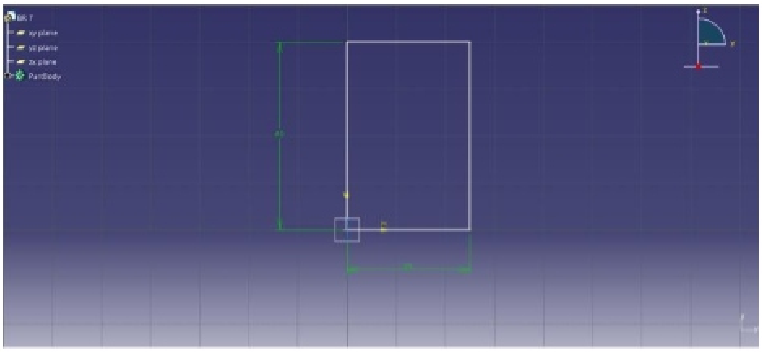

Figure 3.1: Geometrical Representation of Tool Shank in CATIA V5R20

The shank of the tool is obtained by giving PAD to the sketch as shown below

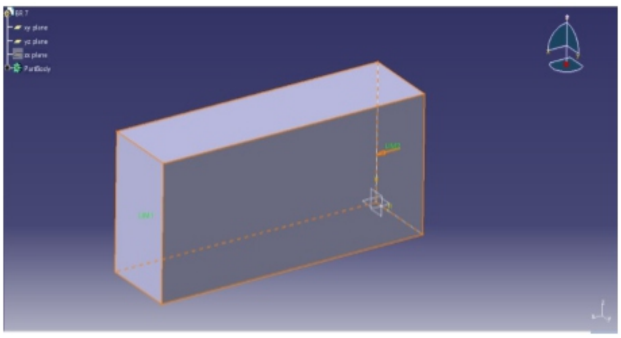

Figure 3.2: Part Model of Shank

ISSN Application No, 21816

The sketch of the tool bit with side rake and side clearance angle is shown below

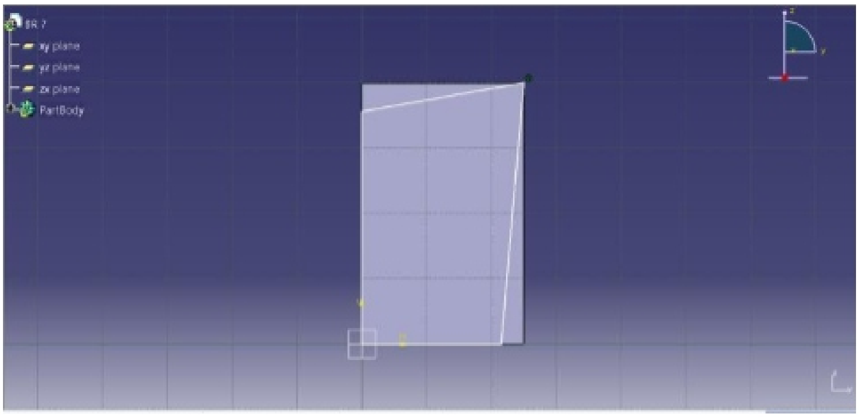

Figure 3.3: Sketch of Tool Bit

The sketch is given PAD command and the obtained is shown below

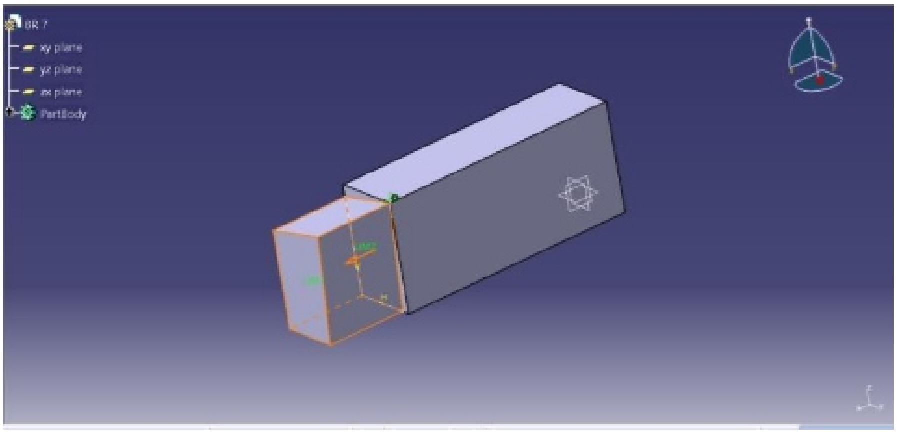

Figure 3.4: Part Model of Tool (Step – I)

The back rake angle is given by using SLOT command and the obtained is shown below

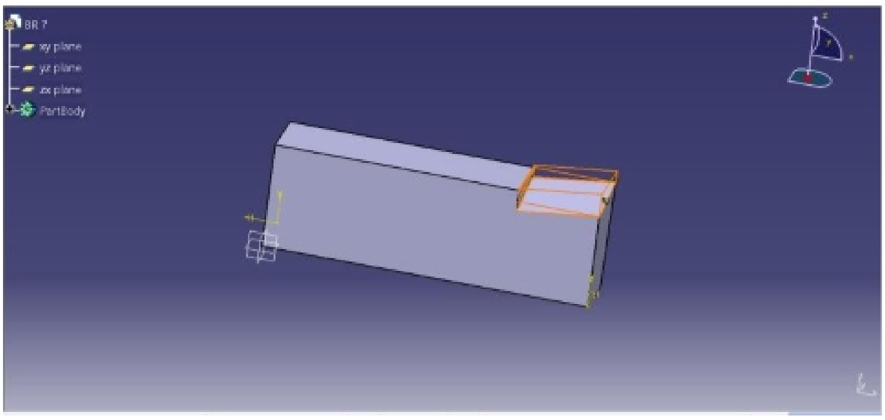

Figure 3.5: Part Model of Tool (Step – II)

The end relief angle is given by using POCKET command and the obtained is shown below

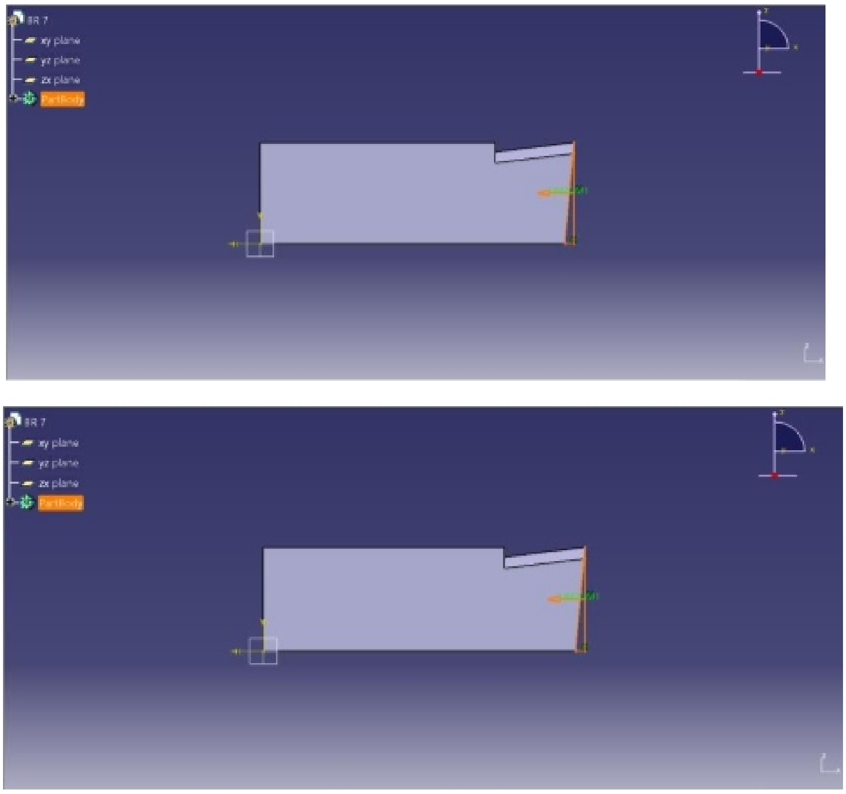

Figure 3.6: Part Model of Tool (Step – III)

The side cutting edge angle is given by using SLOT command and the obtained is shown below

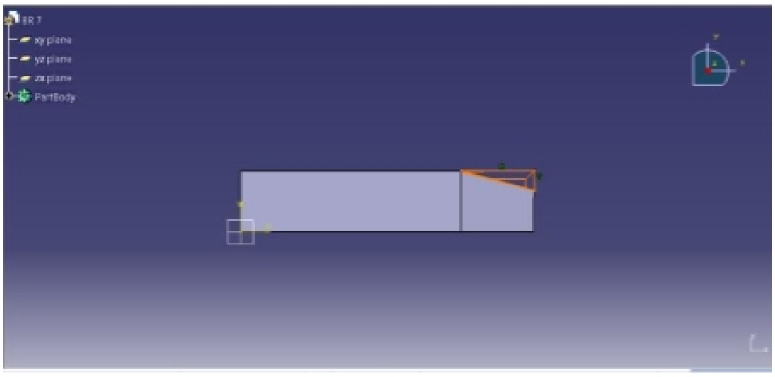

Figure 3.7: Part Model of Tool (Step – IV)

The end cutting edge angle is given by using SLOT command and the obtained is shown below

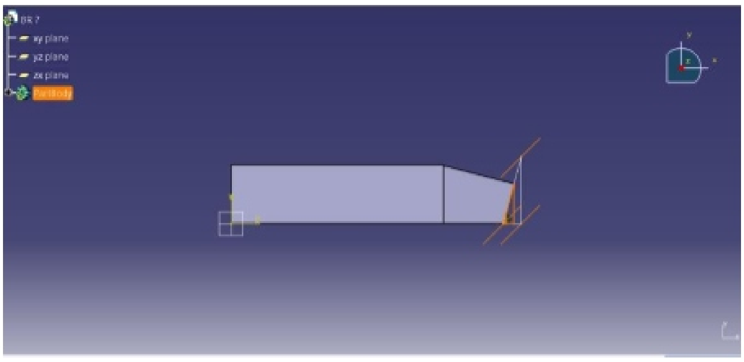

Figure 3.8: Part Model of Tool (Step – V)

The Tool modelled in CATIA software is shown below

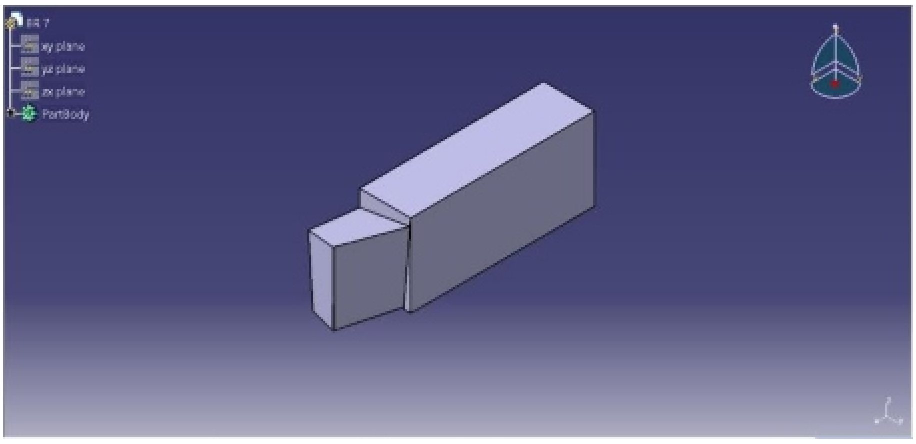

Figure 3.9: Designed Tool with Back Rake Angle 7^0

Similarly three more tools are designed in CATIA software by varying Back Rake angle (7^0, 8^0, 9^0, and 10^0) as shown in fig. below respectively

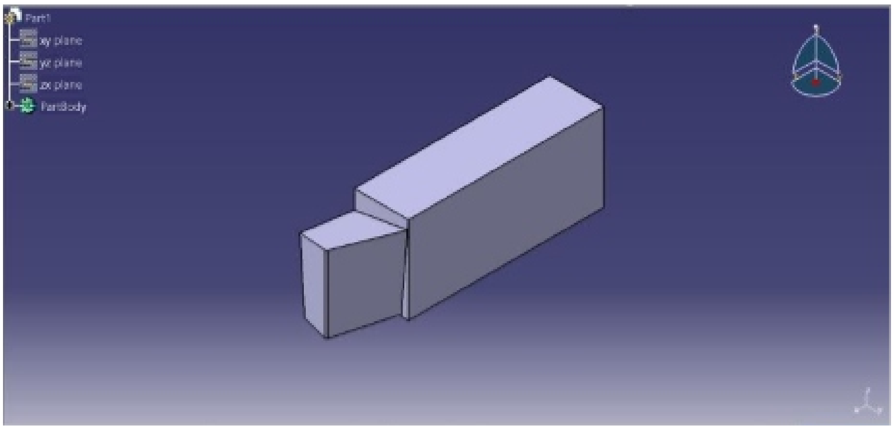

Figure 3.10: Designed Tool with Back Rake Angle 8^0

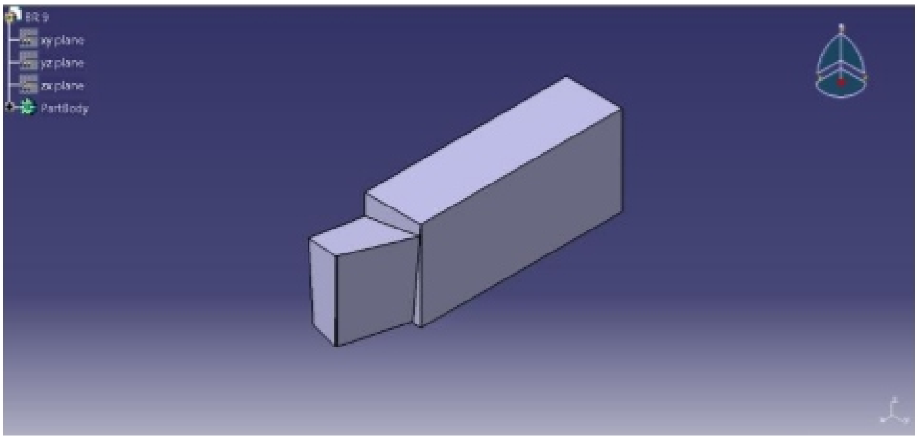

Figure 3.11: Designed Tool with Back Rake Angle 9^0

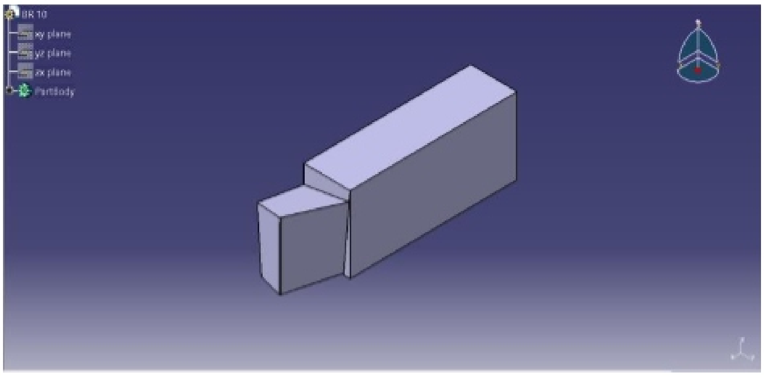

Figure 3.12: Designed Tool with Back Rake Angle 10^0

Anlysis of tool

All the models dawn in Catia are imported into Ansys in .igs format and analysis is done by varying speed, feed and depth of cut, various forces acting on the single point cutting tool are obtained. The various forces thus obtained are used for determining the von-mises stress, von- mises strain and deformation. Analysis of the tool is done in the Static Structural Module.

Engineering Data

In Engineering Data, the materials and their properties are taken into consideration. For the project, 8-4-1 High Speed Steel and Cemented Carbide are considered.

The material properties for 8-4-1 HSS are as follow:

Table 4.1: Material Properties of 8-4-1 HSS:

Density	8160 kg/m^3
Young's Modulus	210 GPa
Poisson's Ratio	0.3
Yield Strength	3250 MPa

The material properties of Cemented Carbide are as follows:

Table 4.2: Material Properties of Cemented Carbide

Density	15630 kg/m^3
Young's Modulus	550 GPa
Poisson's Ratio	0.234
Ultimate Strength	3448 MPa

Geometry:

The part modelling of CATIA file is saved in the '.igs' format and then imported to Static Structural Module.

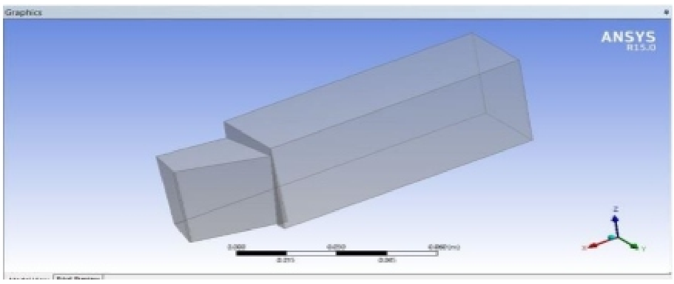

Figure 4.1: Geometry

Model:

The imported file geometry undergoes meshing, after which the physics is defined to theexternal domain. Fine Mesh is considered for good results

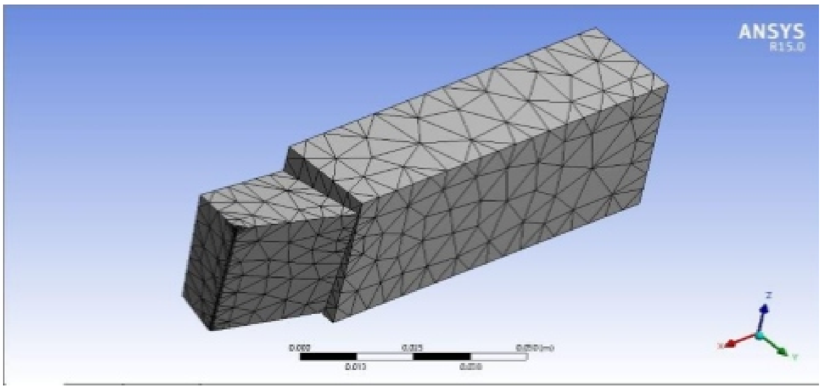

Figure 4.2: Meshing

Boundary Conditions:

The Boundary conditions for the tool are defined as follows: The shank of the tool is fixed and the figure is shown below

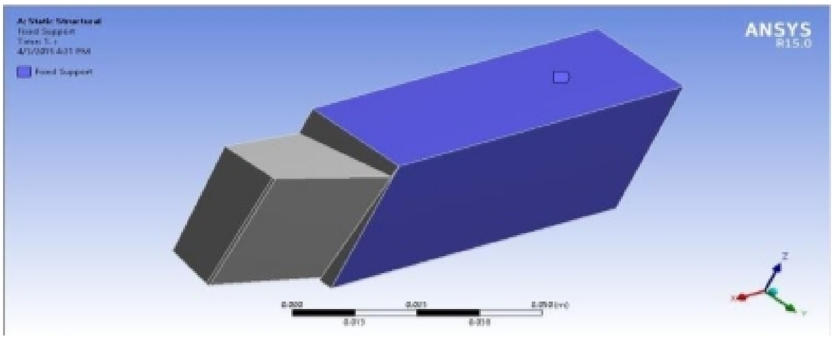

Figure 4.3: Fixed Support

Iteration No.	Speed (RPM)	Feed (mm/rev)	Depth of Cut (mm)	Forces (N)		
				Cutting Force	Feed Force	Radial Force
I	269	0.094	0.5	167.58	116.739	48.069
II	269	0.38	1	916.254	619.01	309.996
III	269	0.69	1.5	1084.986	811.287	509.139
IV	315	0.094	0.5	453.2	412.02	279.59
V	315	0.38	1	1013.73	902.52	146.169
VI	315	0.69	1.5	307.053	232.49	115.75
VII	525	0.094	0.5	631.764	559.17	243.288
VIII	525	0.38	1	247.212	164.808	103.986
IX	525	0.69	1.5	1092.834	813.249	471.861

Table 4.3: Boundary Conditions

The forces are given at the tip of the tool and it is shown in the ANSYS MECHANICAL tool below:

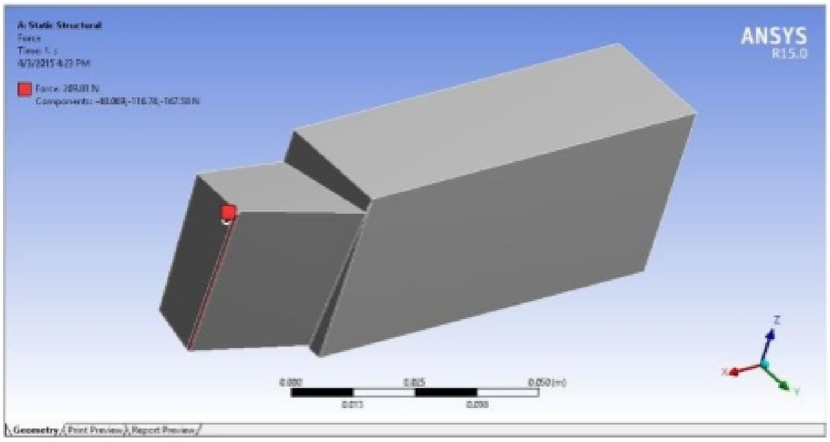

Figure 4.4: Boundary Conditions

Solutions and Results:

After applying the boundary conditions, the solutions and results for 8-4-1 HSS and cement carbides are as follows:

Results and discussion

Results of 8-4-1 HSS Tool:

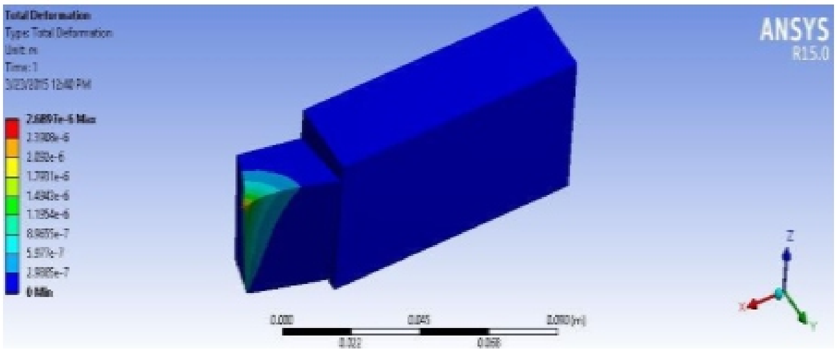

Figure 5.1: Deformation at 90 (Iteration – IX)

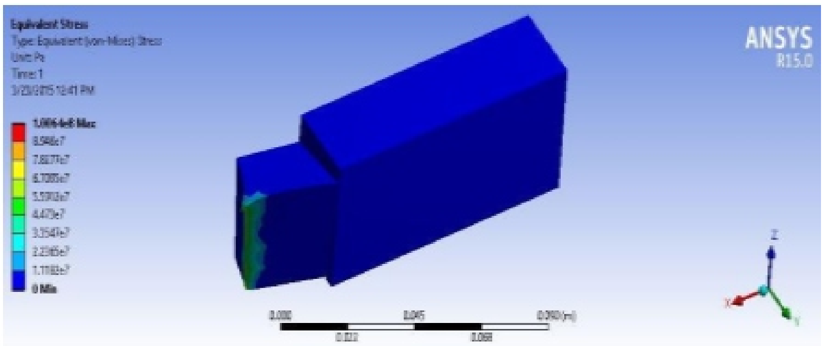

Figure 5.2: Stress at 90 (Iteration – IX)

Results of Cemented Carbide Tool:

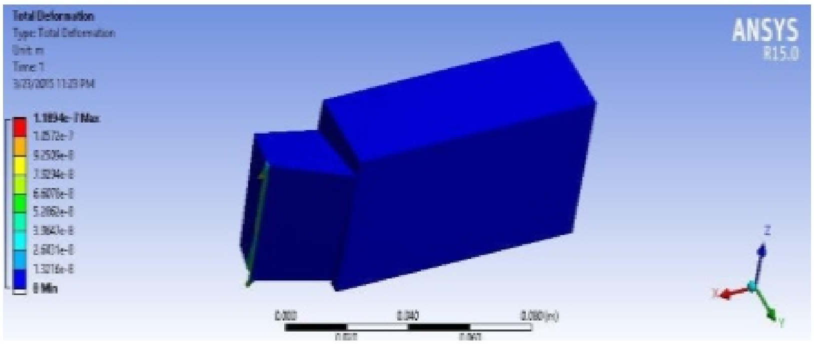

Figure 5.3: Deformation at 90 (Iteration – IX)

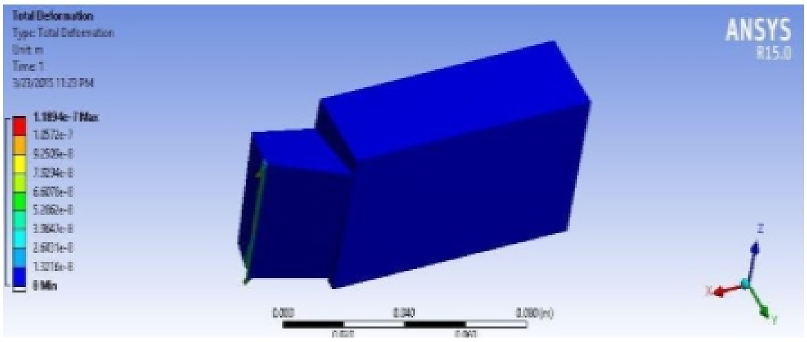

Figure 5.4: Stress at 90 (Iteration – IX)

RESULTS:

The results from the static structural analysis on the single point cutting tool using ANSYS are tabulated and are shown as follows:

Results and graphs of 8-4-1 HSS tool:

Iteration No.	FORCES	Stress (Pa)			
		Back Rake angle 7^0	Back Rake angle 8^0	Back Rake angle 9^0	Back Rake angle 10^0
I	206	1599.486	1580.203	1720.069	1658.109
II	313.92	2281.675	2262.443	2423.121	2333.525
III	402.21	2971.911	2893.007	3162.251	3046.008
IV	667.08	4379.904	4299.658	4729.231	4667.593
V	873.09	6380.027	6300.536	6907.801	6899.157
VI	1147.77	8499.965	8439.352	9189.895	9188.899
VII	1363.59	9009.356	8993.657	9503.256	9450.125
VIII	1442.07	10086.035	10078.887	10396.895	10247.153
IX	1451.88	10144.638	10060.402	10979.486	10973.349

Table 5.1: Stress values of 8-4-1 HSS tool

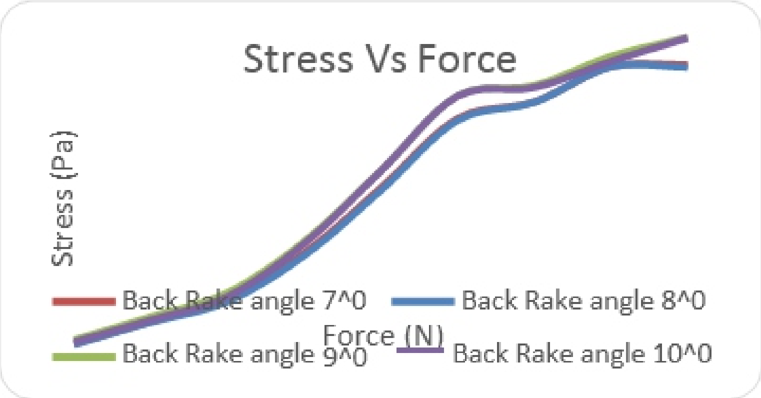

Figure 5.1: Stress vs Force for 8-4-1 HSS tool at different Back Rake angles

Iteration No.	FORCES	Deformation (mm)			
		Back Rake angle 7^0	Back Rake angle 8^0	Back Rake angle 9^0	Back Rake angle 10^0
I	206	0.00379	0.00368	0.00398	0.00411
II	313.92	0.00434	0.00419	0.00459	0.00476
III	402.21	0.00572	0.00554	0.00578	0.00583
IV	667.08	0.00606	0.00597	0.00613	0.00639
V	873.09	0.0065	0.00649	0.00697	0.00715
VI	1147.77	0.00689	0.00673	0.00719	0.00735
VII	1363.59	0.00709	0.00705	0.00742	0.00741
VIII	1442.07	0.00719	0.00718	0.00759	0.00761
IX	1451.88	0.00732	0.00723	0.00771	0.00779

Table 5.2: Deformation values of 8-4-1 HSS tool

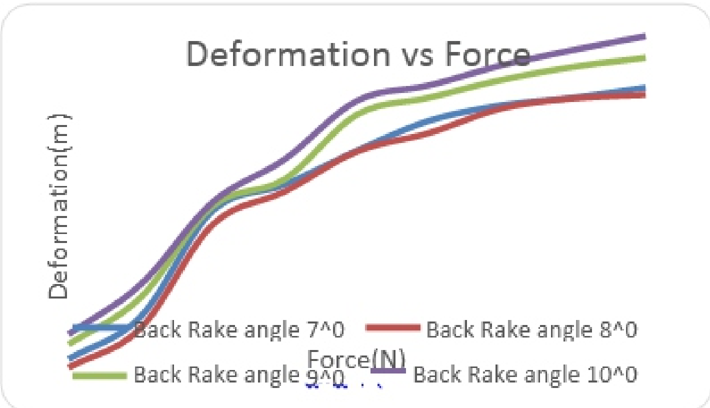

Deformation(m)Figure 5.2: Deformation vs Force for 8-4-1 HSS Tool at different Back Rake angles

Results and graphs of Cemented Carbide tool

teration No.	FORCES	Stress (Pa)			
		Back Rake angle 7^0	Back Rake angle 8^0	Back Rake angle 9^0	Back Rake angle 10^0
I	206	1616.217	1809.444	1827.758	1850.787
II	313.92	2255.006	2528.287	2551.865	2582.461
III	402.21	2987.338	3276.739	3308.871	3349.117

IV	667.08	4569.993	4692.931	4734.823	4787.242
V	873.09	6639.565	6999.371	7099.445	7154.873
VI	1147.77	8592.884	9437.405	9851.262	9871.891
VII	1363.59	9023.159	9756.482	10457.486	10305.446
VIII	1442.07	10134.124	10306.483	10636.49	10505.456
IX	1451.88	10312.427	10514.257	10879.486	10790.473

Table 5.4: Stress values of Cemented Carbide tool

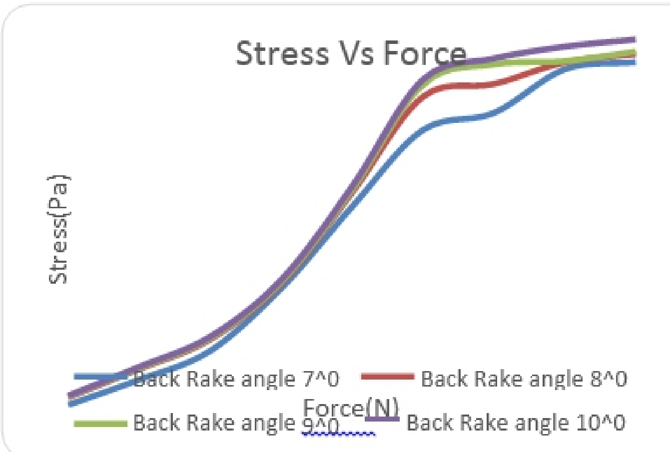

Figure 5.3: Stress vs Force for Cemented Carbide Tool at different Back Rake angles

	FORCES	Deformation (mm)			
Iteration No.		Back Rake angle 7^0	Back Rake angle 8^0	Back Rake angle 9^0	Back Rake angle 10^0
I	206	0.00145	0.00061	0.00054	0.000535
II	313.92	0.00206	0.0009	0.000878	0.000823
III	402.21	0.00259	0.00134	0.00112	0.00105
IV	667.08	0.00352	0.00199	0.00181	0.00164
V	873.09	0.00434	0.00259	0.0024	0.00224
VI	1147.77	0.00583	0.00364	0.00322	0.0031
VII	1363.59	0.00654	0.00423	0.00386	0.00364
VIII	1442.07	0.00704	0.00499	0.00432	0.0042
IX	1451.88	0.00722	0.00564	0.00521	0.00499

Table 6.6 Deformation values of Cemented Carbide tool

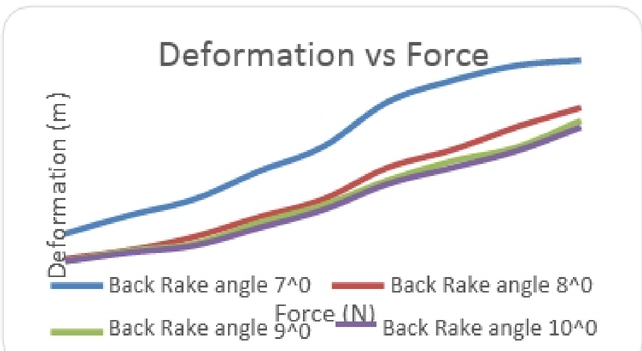

Figure 5.4: Deformation vs Force of Cemented Carbide Tool at different Back Rake angles

CONCLUSIONS

- The optimal tool geometry had more tool life than the basic tool. Depth of Cut has greatest influence on cutting force, followed by feed, while cutting speed has least influence.
- The temperature at the tip of the cutting tool during the time of machining is influenced by cutting speed
- It is observed as the cutting angles are increased the area throughout the body of the tool decreases, and the stress increases.
- Optimal angle is taken at the point of maximum stress obtained because maximum stress condition is observed at lower cross sectional area of tool tip while deformation produced by the tool in the work material is less at lower cross sectional area of the tool tip due to which the less cutting are generated and the heat generated by the tool will be less.
- For 8-4-1 HSS and Cemented Carbide the maximum stress condition was achieved at a Back Rake Angle of 90, when compared between Back Rake Angles 70,80, 90 and 100.
- When comparing across tool materials, by taking all the properties into account cemented carbide steel is best material.

REFERENCES

[1].RoopsandeepBammidi and Prathyusha, "Optimization of Single Point Cutting Tool", International Journal of Engineering Research & Technology, Vol-3, Issue 5, May – 2014.

[2]. S. Sundaram, P. Senthilkumar, A. Kumaravel and N. Manoharan, "Study Of Flank Wear In Single Point Cutting Tool Using Acoustic Emission Sensor Techniques", ARPN Journal of Engineering and Applied Sciences, VOL. 3, NO. 4, AUGUST 2008

[3]. K. Kadirgama, K. A. Abou-El-Hossein, B. Mohammad, M. M. Noor and S. M. Sapuan, "Prediction of tool life by statistic method in end-milling operation", Scientific Research and Essay, Vol. 3 (5), pp. 180-186, May, 2008

[4]. S. Dolinsek, J. Kopac, "Mechanism and types of tool wear; particularities in advanced cutting materials", Journal of Achievements in Materials and Manufacturing Engineering, VOLUME 19, ISSUE 1, November 2006

[5]. W.S. Lin, "The reliability analysis of cutting tools in the HSM processes", Archives of Materials Science and Engineering, Volume 30, Issue 2, April 2008, Pages 97-100

[6].Prasanna P Kulkarni, Shreelakshmi.C.T.,Shruti.V.Harihar, RadhaBai.N. "An Experimental Investigation of Effect of Cutting Fluids on Chip Formation and Cycle Time in Turning of EN- 24 and EN-31 Material", IJSER (ISSN:2277-9655) Nov – 2014, PP: 574-582.*

[7].Ajit Kumar Senapathi, AbhijitBhatta and AvinashSenapathi, GIET, India, "Effect of Machining Parameters on Cutting forces during Turning of Mild Steel on High Speed Lathe by using Taguchi Orthogonal Array", Global Journal of Advanced research, Vol-1, Issue 1.

[8].DeeepakLathwal and Deepak Bhardwaj, "Study and Analysis of Single Point Cutting Tool under Variable Rake angle", International Journal for Research in Applied Science and Engineering Technology, Vol-1, Issue 1, August 2013

[9].S.H.Rathod and Mohd. Razik, "Finite Element Analysis of Single Point Cutting Tool"International Journal Of Modern Engineering Research (IJMER)

[10].Dr.Toshimichi MORIWAKI, Professor Department of Mechanical Engineering, KOBE University, "Trends in Recent Machine Tool Technologies"

[11].S.R.Das and R.P.Nayak, "Optimization of Cutting Parameters on Tool Wear and Work piece surface temperature in turning of AISI D2 STEEL" , International Journal of Lean Thinking, Volume 3,Issue 2(December 2012)

Design and Farication of Industrial Parameter Monitoring and control Robot

CH Uma Chaithanya[*], K Sri Ram Murthy[**], P Siva Vasu[***], D Rama Krushna [****], K Yuva Kishore[*****], K P Bala Krishna[******]

[*]Doctorate Program, Linguistics Program Studies, Udayana University Denpasar, Bali-Indonesia (9 pt), Assistant Professor, Department Of Mecanical Engg, BITS-Vizag, India

Email: uma.nitw@gmail.com

** STIMIK STIKOM-Bali, Renon, Depasar, Bali-Indonesia

*** English Language Specialist, Oller Center, Carriage House, 2nd Floor, California, USA

**** Head, Dept. of Political Science, Faculty of Arts & Culture, South Eastern University of Sri Lanka, Oluvil, Sri Lanka

A B S T R A C T

Now-a-days the accidents in the coal mine industries have increased. Even if any explosion occurs it can't be easily known to the worker and it may cause accidents. So in order to avoid this, a robot has been designed and this robot is allowed to monitor the ambient situations inside the coal mine industry. Some of the environmental parameters such as methane leakage, temperature, oxygen are sensed by using the high end sensors and the sensed data are transmitted for monitoring the status of the coal mine and to control the robot movement.

If the temperature exceeds a threshold, the cooling fan is automatically set to ON and if any gas leakage is detected the workers are given alert through a buzzer. By this the human intervention can be avoided inside the industry and the accidents can be prevented.

Keywords: DC Motors; Sensors; Buzzer; Battery;

1. INTRODUCTION

In the hazardous working environment, human safety is an important concern. Coal mines is a place in which human lives are more dangerous and many workers are injured due to explosions and leakage of toxic gases. Fire accidents can also happen. At the same time if any person is absent in an important place for monitoring, it may also cause serious hazards. At present many systems are implemented in industrial areas but still those accidents are occurring. The new method is to design a robot and that robot is allowed to enter into the coal mine area. The robot will be equipped with some sensors like temperature and gas for detecting the toxic gases and the ambient temperature.

The robot used must be a flame-proof so that even if any disaster occurs it will transmit the information to the receiver without fail. Also, it must be designed to work in the high temperature situations. If any serious situation occurs means an alert given to the nearby workers. Wireless communication is also an important issue inside the industry Usage of wired technologies are not worthy as the cables will get damaged after a certain period of time or due to some environmental factors. So the wireless transmission technology is preferred. The industrial monitoring protocol should be designed such that the system must have a reliable end to end data delivery. The data which is collected from the robot should be transmitted without any delay and loss of data.

2. RESEARCH METHOD

2.1. HARDWARE IMPLEMENTATION

The Raspberry pi 2 microprocessor is used since this is compact in size and the power consumption is too low. Broadcom chip BCM2836 SoC is placed in it and it has a memory of 1GB RAM with 900MHz frequency. Raspberry Pi 2 board is selected because it is fast when compared to the earlier versions. Many sensors or peripherals can be interfaced with it at the same time and can work very fast as the quad core processor is used in it. This processor allows us to interface many modules at a time.

The temperature sensor used here is DS18B20. As it is a digital sensor it is easy to interface with the raspberry pi board. It is used to sense the ambient temperature of the coal mine industry. This sensor is connected with the GPIO pins. The working of the cooling fan depends on the above sensed data. DS18B20 sensor has an operating range of about 55ºC to 125ºC. Inside the industrial area the temperature may exceed above 45ºC. So this sensor is used. MQ3 gas sensor is used in order to sense the gas leakage in the mining areas.

A gas sensor is for detecting the combustible, flammable and the toxic gases. The MQ3 sensor mainly detects the methane gas which is most emitted in coal mining areas. The voltage required is 5V which is provided from the GPIO pin. In the gas sensor, H-pins are allowed to heat for a while so that it can detect the gas. Once the gas is detected, an alert is given to the workers.

2.2. TECHNICAL DATA BUZZER:

A buzzer is an audio signaling device, which may be Mechanical, Electro mechanical, or piezoelectric. Typical uses of buzzers and beepers include alarm devices, timers, and confirmation of user input such as a mouse click or keystroke. A buzzer is an electrical device that is used to make a buzzing sound, for example, to attract someone's attention.

Fig.1

DC MOTORS:

A direct current or DC motor convert's electrical energy into mechanical energy. It is one of two basic types of motors: the other type is the alternating current or AC motor. Among DC motors, there are shunt-wound series-wound, compound-wound and permanent magnet motors.

FUNCTION:

A DC motor consists of a stator, an armature, a rotor and a commutator with brushes. Opposite polarity between the two magnetic fields inside the motor cause it to turn. DC motors are the simplest type of motor and are used in household appliances, such as electric razors, and in electric windows in cars.

BASIC DC MOTOR OPERATION:
A DC motor is equipped with magnets, either permanent magnets or electromagnetic windings that produce a magnetic field. When current passes through the armature, also known as the coil or wire, placed between the north and south poles of the magnet, the field generated by the armature interacts with the field from the magnet and applies torque. In a DC motor, the magnet forms the stator, the armature is placed on the rotor and a commutator switches the current flow from one coil to the other. The commutator connects the stationary power source to the armature through the use of brushes or conductive rods. Furthermore, DC motors operate at a fixed speed for a fixed voltage and there is no slip.

Fig. 2

SENSORS:
In the broadest definition, a sensor is an electronic component, module, or subsystem whose purpose is to detect events or changes in its environment and send the information to other electronics, frequently a computer processor. A sensor is always used with other electronics, whether as simple as a light or as complex as a computer.

TYPES OF SENSORS FOR MAKING ROBOT

1. INFRARED SENSOR:
An Infrared sensor is an electronic sensor that measures Infrared (IR) light radiating from objects its field of view. They are most often used in IR-based motion detectors.

PRINCIPLE OF OPERATION:
We have already discussed how a light sensor works. IR Sensors work by using a specific light sensor to detect a select light wavelength in the Infra-Red (IR) spectrum. By using an LED which produces light at the same wavelength as what the sensor is looking for, you can look at the intensity of the received light. When an object is close to the sensor, the light from the LED bounces off the object and into the light sensor.

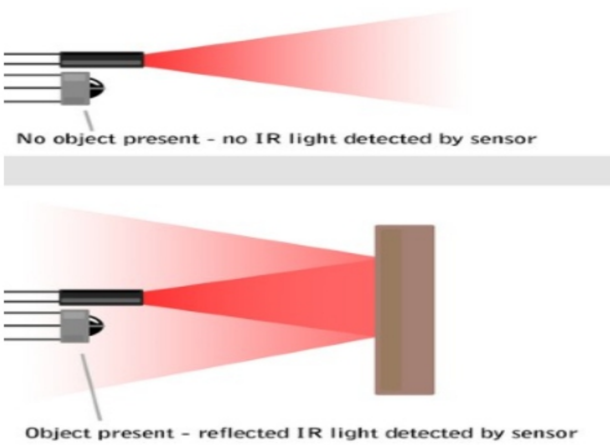

Fig.3

2. TEMPERATURE SENSOR:

Temperature is the most often-measured environmental quantity. This might be expected since most physical, electronic, chemical, mechanical, and biological systems are affected by temperature. Certain chemical reactions, biological processes, and even electronic circuits perform best within limited temperature ranges. Temperature is one of the most commonly measured variables and it is therefore not surprising that there are many ways of sensing it. Temperature sensing can be done either through direct contact with the heating source, or remotely, without direct contact with the source using radiated energy instead. There are a wide variety of temperature sensors on the market today, including Thermocouples, Resistance Temperature Detectors (RTDs), Thermostats, Infrared, and Semiconductor Sensors.

Fig. 4

3. GAS SENSOR:

In current technology scenario, monitoring of gases produced is very important. From home appliances such as air conditioners to electric chimneys and safety systems at industries monitoring of gases is very crucial. Gas sensors are very important part of such systems. Small like a nose, gas sensors spontaneously react to the gas present, thus keeping the system updated about any alterations that occur in the concentration of molecules at gaseous state.

Gas sensors are available in wide specifications depending on the sensitivity levels, type of gas to be sensed, physical dimensions and numerous other factors. This Insight covers a methane gas sensor that can sense gases such as ammonia which mightget produced from methane. When a gas interacts with this sensor, it is first ionized into its constituents and is then adsorbed by the sensing element.

Fig.5

- MQ3 gas sensor is used in order to sense the gas leakage in the mining areas.
- The voltage required is 5V
- If the gas leakage is sensed, the buzzer will become ON and alert the Surrounding people.

BATTERY:

An electric is a device consisting of one or more electrochemical cells with external connections provided to power electrical devices such as flashlights, smart phones, and electric cars. When a battery is supplying electric power, its positive terminal is the cathode and its negative terminal is the anode. The terminal marked negative is the source of electrons that when connected to an external circuit will flow and deliver energy to an external device.

2.3 IMPLEMENTED SOFTWARE

The raspbian os is used in the raspberry pi board. It is a free operating system that is based on Debian which is particularly optimized for the Raspberry Pi hardware. It comes with over 35,000 packages and pre-compiled software bundled in a simple format for easy installation in the Raspberry Pi. The coding for all the sensors and the robot movement are done using the python coding. Python is preferred since it is a simple and a minimalistic language. It is also free and open source software. This can be used in many platforms such as Linux, VxWorks, and Pocket PC etc. Also, it supports procedure-oriented programming as well as OOPS. The web browser is created by using HTML.

PROPOSED WORK:

A robot is designed using the raspberry pi board. The raspberry pi board is given a power supply of about 5V. The sensors which are connected are given power through the GPIO pins. An ALERT button is placed at the centre for giving alert to the workers in case of any emergency. The robot wheels are given 12V from a separate rechargeable battery. The movement of the robot depends on the python coding inside the raspbian os. The wheels are connected through a relay. The relay which here used is a 4-channel relay. When the robot is kept stationary, the GPIO pin which is connected to that particular relay is given high. During movement they are set to low. When the temperature sensor senses the temperature above 35ºC, Also, when any gas is sensed, the GPIO pin of the buzzer is kept low and thus the buzzer will be ON. If there is more suffocation inside the mining area, the carbon dioxide emission will be more. When this CO_2 is sensed, the oxygen supply cylinder will be opened by setting the GPIO pin of that particular relay to low. For giving alert the audio and if any emergency situation occurs the ALERT button is pressed and thus the sound will be produced

Block Diagram

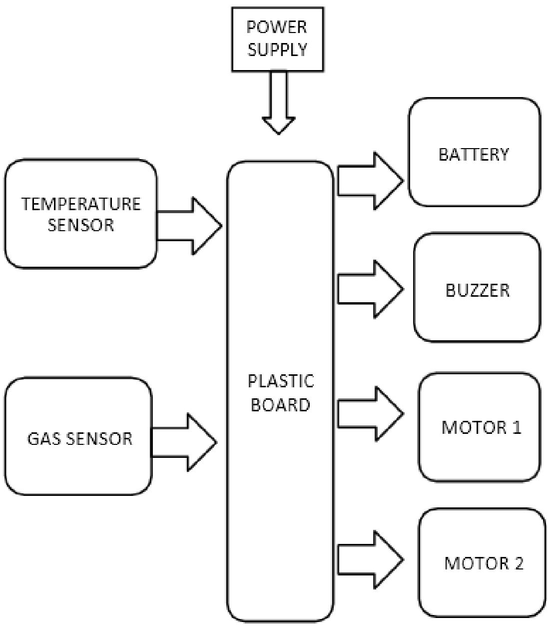

Block diagram of industrial parameter monitoring and control robot

3. RESULTS AND ANALYSIS

The following are the experimental results. The Figure shows the designed robot..The ALERT button is for giving the emergency alert. The live video of the industrial area will be shown in that rectangular window in the centre. The time and date will be shown in the right most corner in the downside. In the emergency area, a person should be always present. If they are absent means, the alert is given through the speaker. The sensed data such as the temperature value, gas sensor value.

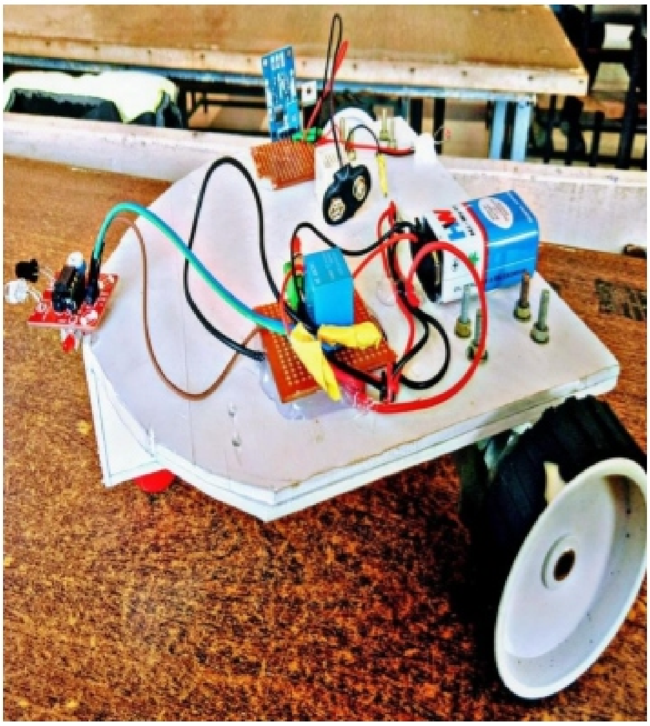

Final model of industrial parameter monitoring and control robot

ADVANTAGES & DISADVANTAGES ADVANTAGES:

- Consistency Of Performance
- 24/7 Continuous Working
- Reduced Amount Of Operator Errors
- Improved Quality Of The Product
- It Can Move From One Location To Another Location
- Robotic Workers Never Get Tired
- Do Not Need To Be Paid
- Can Be Made To Perform Even The Most Dangerous Tasks Without Concern
- Wide Acceptance
- Identify Issues In Real Time, Before They Impact End Users
- Automate Responses To Speed Response Time And Maximized Availability
- Access Critical Data Quickly And Avoid A Lengthy Investigation Process DISADVANTAGES:
- Initial Expensive Development Costs
- Unemployment Due To Many Assembly Line Jobs Now Being Done By Robots/Loss Of Human Jobs
- Possible Need For Extra Space/New Technology To Accommodate Robots
- Cost Of Maintenance /Running Cost Is More

APPLICATION AREAS:

• Exploration , monitoring and surveillance
-Space exploration
-underwater/surface exploration
-Wildlife observation
-Fire awareness monitoring
-Debris cleaning and human rescue
-spy robots

• Household and education
-Household appliances control
-Virtual stimulators and games
-Virtual distance laboratories

• Manipulations from distance ,indirect manipulations
-Bomb diffusion
- Tele surgery
-Nuclear decontamination and decommissioning

4. CONCLUSION

The designed robot is reliable to use and can be used in any working environment. The sensors which are used are so sensitive. The gas sensor will also detect other leakage such as hydrogen, smoke etc. This model can also be used for other purpose also. The suffocation of the working inside the mine is avoided. The accidents are prevented which are caused by ambient conditions.

This application can be used for all industrial area where human intervention for security can be avoided. In hospitals, shopping malls also this application can be used. In case of any fire accidents water has to be sprayed at the right place. Also, some other sensors such as dust sensor, humidity sensor can be interfaced for further convenience of the workers.

REFERENCES

[1] Raguvaran. K, Mr. J. Thiyagarajan "Global Industrial Process Monitoring Through Wireless Communication" in International Conference on Robotics, Automation, Control and Embedded Systems – RACE 2015.

[2] Shushan Hu1,2 ,Cunchen Tang1, Riji Yu1, Feng Liu1, Xiaojun Wang2 "Intelligent Coal Mine Monitoring System based on the Internet of Things" in 978- 1-4799-2860-6/13/$31.00 ©2013 IEEE.

[3] Chen Yan, Song Nan-Nan "The Research of Coal Mine Security Monitoring System Based on Wireless Sensors Network" in Jiangsu Province of China under Grant No.KC0919.

[4] Zing Waxen, "Exploration for Human Factors in the Design of Coalmine Safety and Rescue Devices", IEEE International Conference on Robotics, July 5, 2006.

[5] Zhu Jiangsu, Ago Juneau, Li Katie, Lin Wei, Bi Shogun, "Embedded Control System Design for Coal Mine Detect and Rescue Robot", IEEE, 2010

[6] Li Rung, "A study of the security monitoring system in coal mine underground based on WSN", IEEE,2011

[7] Dr. V. Gomathi, , Ganeshia R , Sowmeya S, Avudaiammal P.S "Design of an Adaptive Coal Mine Rescue Robot using Wireless Sensor Networks" in International Journal of Computer Applications (0975 – 8887) National Conference on Information Processing and Remote Computing, NCIPRC 2015.

[8] Siobhan M. A., A. S. Bide "Study of Unmanned Vehicle (Robot) for Coal Mines" in International Journal of Innovative Research in Advanced Engineering (IJIRAE) ISSN: 2349-2163 Volume 1 Issue 10 (November 2014).

ISSN Application No, 21816

Analysis of Bonded Tubular Single Lap Joints subjected to varying Torsion at constant Pressure

Vikas Ranjan* , Dr. R. R Das**
*Assistant professor, Department of mechanical engineering, Baba institute of technology and sciences, India
** Professor, department of mechanical engineering ISM Dhanbad, India

ABSTRACT

The present research deals with Finite Element Method (FEM) based stress and failure analyses of different types of adhesive bonded tubular joint configurations, viz. Tubular Single Lap Joint (TSLJ) and Tubular Socket Joints (TSJ). The bonded joints have been made with laminated FRP composites and have been subjected to different loading conditions viz. circumferential, axial, and torsion. Suitable APDL codes have been developed using ANSYS 14.0 which is capable of capturing the stresses three dimensionally within the joint region. The developed FE model has been validated with respect to analytical results available in literature and found to be in good agreement. Three-dimensional stresses within the joint and different adherend-adhesive interfaces which in turn play key roles in initiating the failures have been studied in details. Locations prone to adhesion and cohesion failures in the overlap or coupling regions have been identified using Tsai-Wü and Parabolic yield criteria based failure indices. Suitable joint parameters and ply-orientations for the laminated FRP composite joints have been suggested in order to improve the performance and resistance of the bonded tubular structures against failures.

Keywords: Finite Element Method (FEM) Tubular Single Lap Joint (TSLJ), Tubular Socket Joints (TSJ) FibreReinforced Polymer (FRP)

INTRODUCTION

As alternative to conventional engineering materials, Fiber-reinforced polymer (FRP) composites are becoming increasingly popular in the engineering applications. The unique characteristics of FRP, such as their light weight, their resistance to corrosion, high energy absorption, and the lower cost of transportation, erection and maintenance, are very promising in the application of FRP in various engineering fields. Bonded tubular structures made with FRP composites have been common structures in various fields of engineering. Three dimensional stress analyses of these structures under internal pressure and torsion have already been discussed in details in chapters 4 and 5. The purpose of the present chapter is to study the combined effect of internal pressure and torsion on stress distributions and failure within the joint region. Special attention has been devoted to study the effect of torque increase at constant pressure on the failure prone regions.

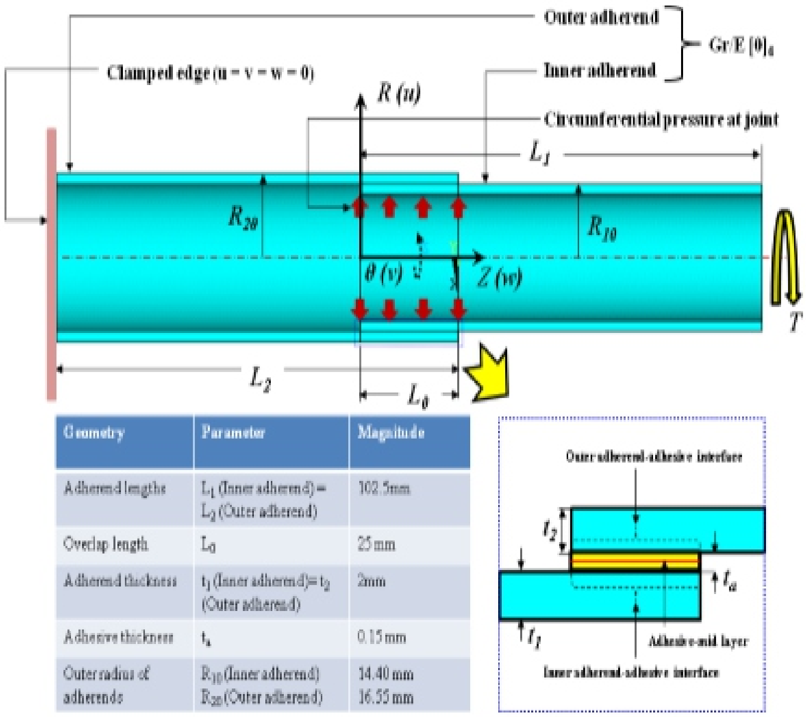

Geometry	Parameter	Magnitude
Adherend lengths	L_1 (Inner adherend) = L_2 (Outer adherend)	102.5mm
Overlap length	L_0	25 mm
Adherend thickness	t_1 (Inner adherend) = t_2 (Outer adherend)	2mm
Adhesive thickness	t_a	0.15 mm
Outer radius of adherends	R_{10} (Inner adherend) R_{20} (Outer adherend)	14.40 mm 16.55 mm

Figure 6.1.Specimen geometry and boundary conditions of the bonded single lap joint along with different interfaces at the joint region.

7.2 Specimen geometry and boundary conditions

Figure 6.1 of the previous chapter shows geometry, configuration, loading and boundary conditions of the bonded TSLJ specimen analyzed in the present study. Two Gr/E [0]4 laminated FRP composite tubes which are similar with respect to length, thickness, and properties have been used as adherends. Here zero degree fiber orientation indicates circumferentially wound fibers. The two tubes have been joined through a thin layer of adhesive (epoxy) as shown in the Figure 6.1. of the previous chapter. The bonded TSLJ have been subjected to an internal pressure of 10 MPa at the inner adherend as well as torsion loading of 100 N-m (direction of the applied torque is CCW as we see from the free end of the bonded TSLJ) at the free end of the bonded TSLJ structure. Torsion loading has been varied as 100 N-m, 110 N-m, 120 N-m, and 130 N-m for a constant internal pressure of 10 MPa in order to study the effect of torsion loading variation on joint strength. The material properties along with strength values for adhesive and adherends have been given in Table 4.1 which have been considered from the work of Das and Pradhan (2010).Three different bondline interfaces have been identified to be the critical regions prone to stress concentration effects in the present analysis: (i) inner adherend-adhesive interface, (ii) adhesive mid-layer, and (iii) outer adherend-adheive interface (Figure 6.1).

7.3 Finite element modelling

The bonded TSLJ has been modelled using the FE codes of ANSYS 14.0. The FE mesh of the bonded TSLJ specimen has been shown in Figure 4.2. The modelling and simulation techniques have already been explained in previous chapters (chapter 3 and 4)

7.4 Results and discussion

Three dimensional stress distributions within the joint region of the bonded TSLJ have been studied in details for pure internal pressure loading and pure torsional loadings in chapters 4 and 5, respectively. In the present chapter effect of torsion loading on the stress distributions within the joint region is intended to be studied when the bonded TSLJ is already under the application of an internal pressure loading at the inner adherend. Effect of torsion loading (100 N-m) on stress distributions and failure indices at different bondline interfaces of the bonded TSLJ subjected to internal pressure loading of 10 MPa has been studied in the first phase of the analysis. Thereafter, the torsion loading has been increased as: 100N-m, 110N-m, 120 N-m, and 130 N- m for a constant internal pressure of 10 MPa and effects have been studied corresponding to the critical bondline interface.

7.4.1 Effect of Torque in presence of Internal Pressure on stresses in joint

7.4.1.1 Inner adherend-adhesive interface

It has already been observed in chapter 4 (Figure 4.3) that under influence of internal pressure, four stress components (σr, σθ, σz, and τrz) at the inner adherend-adhesive interface are of considerable magnitude. Whereas, the rest shear stress components (τrθ, τθz) are of negligible magnitudes. However, for a pure torsional loading, an exactly opposite scenario has been observed. In this case, the negligible stress components in case of pure pressure loading (τrθ, τθz) becomes the most prominent stress components (Figure 5.2 (d), (e)).

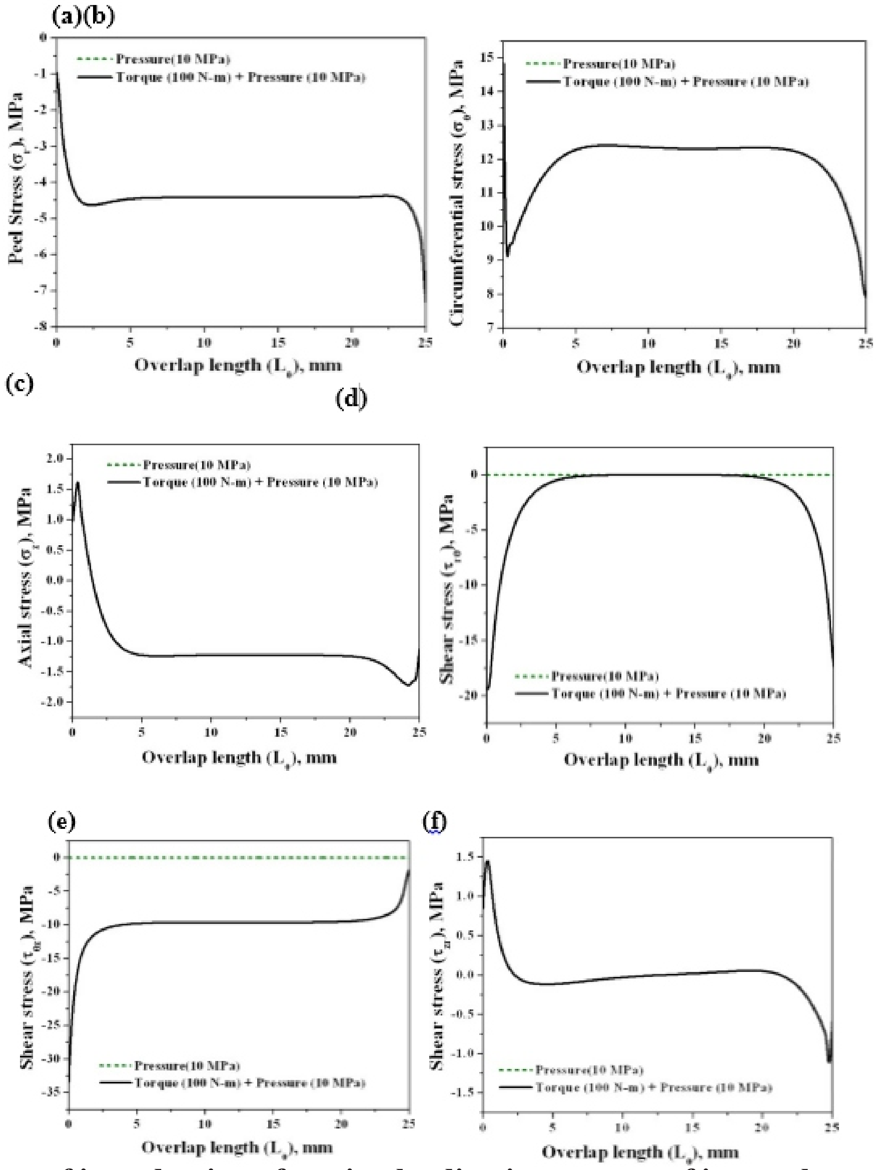

Figure.7.1. Effect of introduction of torsion loading in presence of internal pressure on stress distributions at the inner adherend-adhesive interface.

Whereas, the most prominent stress components for pure pressure loading (σr, σθ, σz, and τrz) are of negligible magnitudes as already explained in chapter 5 through Fugures 5.2 (a), (b), (c), and (f). The present case is just a superposition of these two cases.

The stress distributions also seem to be following a superposition trend as seen from the below figures. Introduction of torsional loading in the joint region enhances the magnitude of shear stresses (τrθ) and (τθz) within the inner adherend-adhesive interface of the bonded TSLJ (Figure 7.1 (d) and (e)). It could be clearly observed that the profile of these stresses (τrθ and τθz) matches exactly with the corresponding stress profiles for pure pressure loading case (Figure 5.2 (d) and (e)). This confirms that the stress distributions follow the superposition principle. Similarly the normal stress profiles (σr, σθ, and σz) and one shear stress profile (τrz) have been observed to be unaffected due to introduction of torsional loading in presence of the internal pressure. The stress profiles again match exactly with the profiles corresponding to pure internal pressure loading case (Figure 4.3 (a), (b), (c) and (f)) confirming the superposition principle again.

7.4.1.2 Adhesive mid-layer

(a)(b)

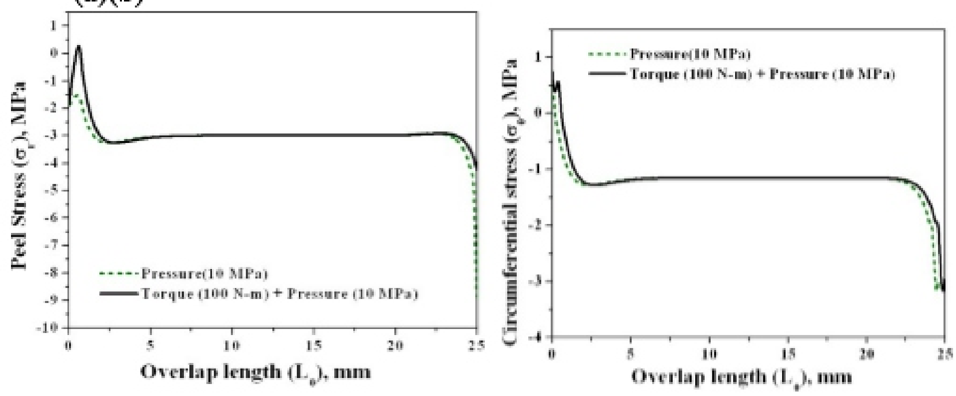

(c) (d)

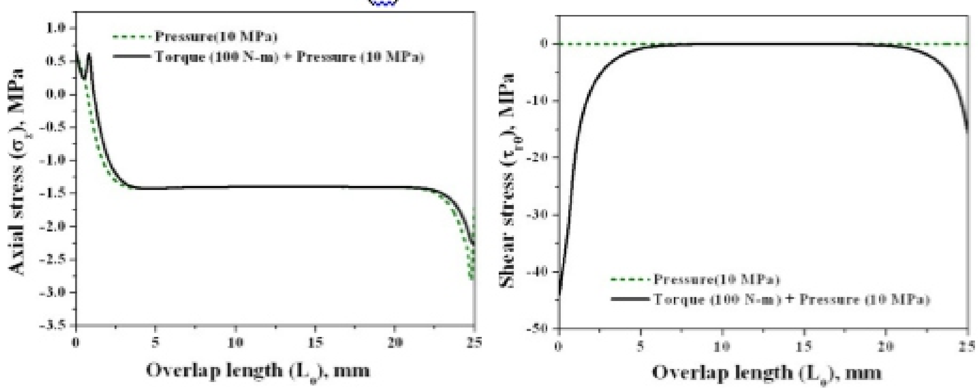

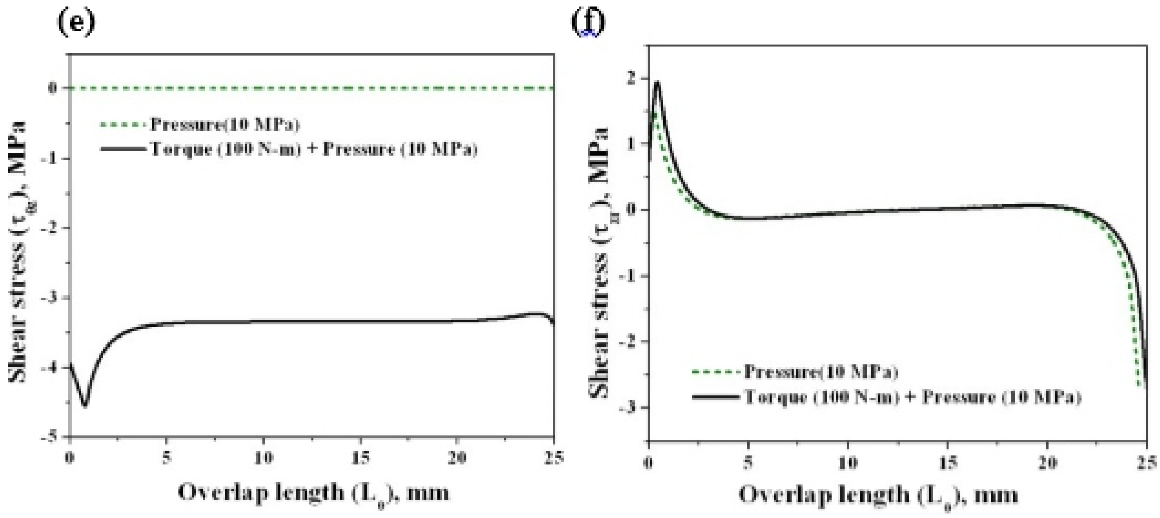

Figure.7.2. Effect of introduction of torsion loading in presence of internal pressure on stress distributions at the adhesive mid-layer.

Introduction of torsional loading of 100 N-m in the joint region enhances the magnitude of shear stresses (τrθ and τθz) within the adhesive mid-layer of the bonded TSLJ (Figure 7.2 (d) and (e)). It could be clearly observed that the profile of these stresses (τrθ and τθz) matches exactly with the corresponding stress profiles for pure torsion loading case (Figure 5.3 (d) and (e)). This confirms that the stress distributions follow the superposition principle. However, the normal stress profiles (σr, σθ, and σz) and one shear stress (τrz) have been observed to be slightly affected due to introduction of torsional loading in presence of the internal pressure loading confirming slight deviation from the superposition principle.

7.4.1.3 Outer adherend-adhesive interface

When a torsion loading of 100 N-m has been introduced in the joint region in presence of internal pressure loading acting at inner adherend of the bonded TSLJ, it enhances the magnitude of shear stresses (τ rθ and τθz) within the outer adherend-adhesive interface (Figure 7.3 (d) and (e)). It could be clearly observed that the profile of these stresses (τrθ and τθz) matches exactly with the corresponding stress profiles for pure torsion loading case (Figure 5.4 (d), and (e)). This confirms that the stress distributions follow the superposition principle. Similarly the normal stress profiles (σr, σθ, and σz) and shear stress (τrz) have been observed to be unaffected due to introduction of torsion loading in presence of the internal pressure loading.

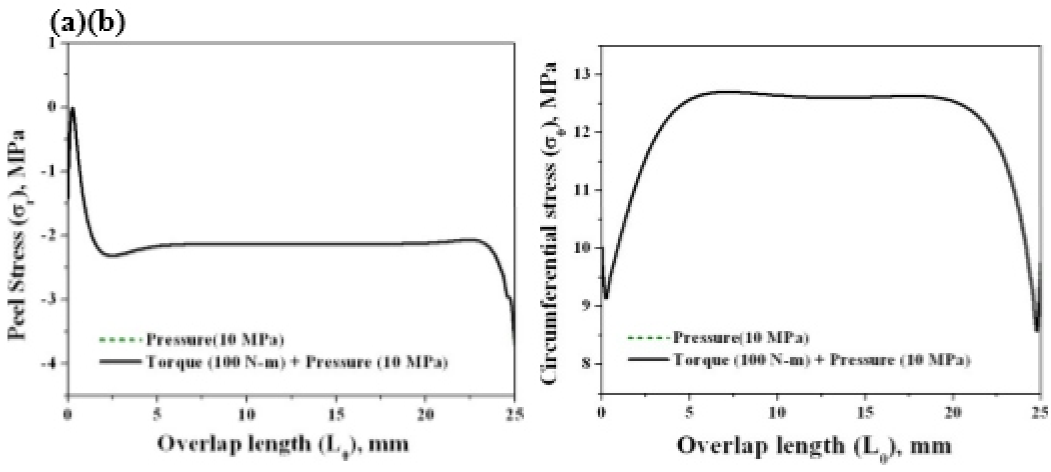

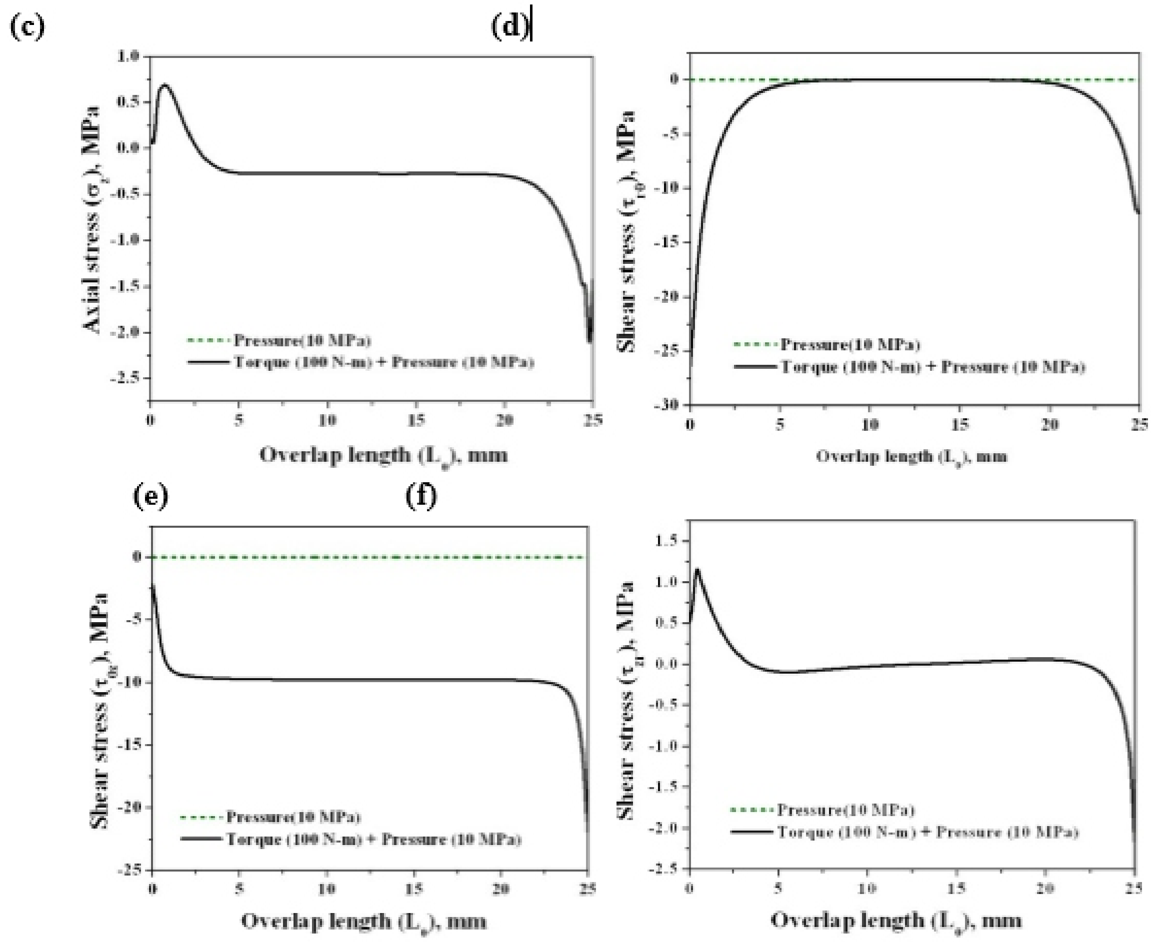

Figure.7.3. Effect of introduction of torsion loading in presence of internal pressure on stress distributions at the outer adherend-adhesive interface.

The stress profiles again match exactly with the profiles corresponding to pure internal pressure loading case (Figure 4.5 (a), (b), (c) and (f)) confirming the superposition principle.

7.4.2 Effect of torsional loading in presence of internal pressure on failure within joint

The failure index profiles for all the bondline interfaces shown in Figure 7 .4 (a), (b), and (c) are completely varying as compared to the failure index profiles corresponding to pure internal pressure as shown in chapter 4 (Figure 4.7). This indicates that introduction of torsion loading along with the internal pressure loading is very much affecting the failure index profiles for the different bondline interfaces. It is important to note here that when the bonded TSLJ is subjected to a combination of torsional and pressure loading, effect of torsional loading is predominantly observed on the failure effects within the joint region. Although the internal pressure loading has been observed to be affecting major stress components within the joint region, still it is unable to have a prominent effect as far as failure within the joint region is concerned.

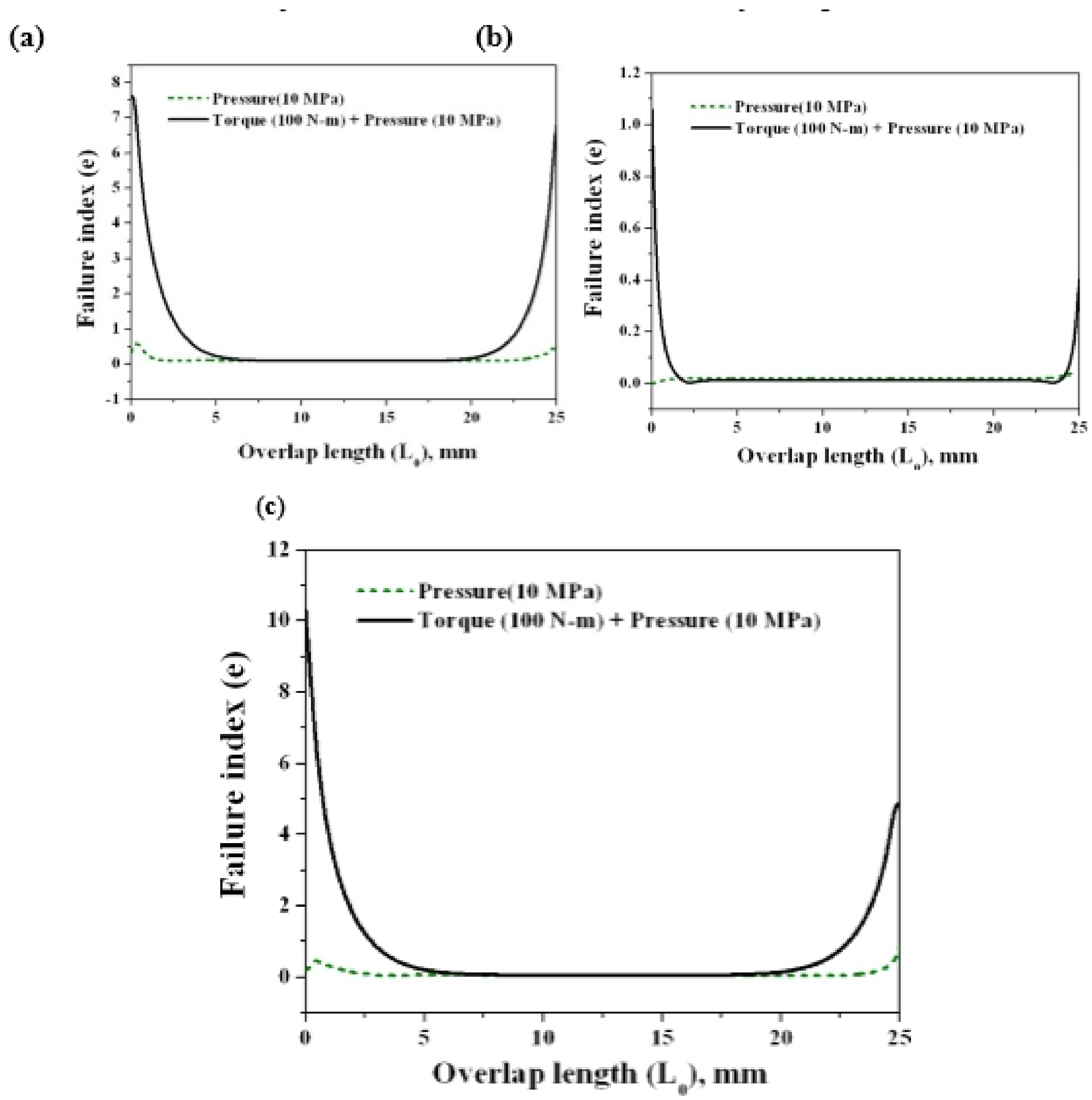

Figure.7.4. Effect of introduction of torsional loading in presence of internal pressure on failure indices at different bondline interfaces: (a) inner adherend-adhesive interface, (b) adhesive mid-layer, and (c) outer adherend-adhesive interface.

This has been clearly observed in Figure 6.5 of chapter 6, where it can be clearly observed that the failure index profiles at all the bondline interfaces match exactly with the failure index profiles for a pure torsional loading case. This indicates that application of pressure with respect to torsional loading does not affect the magnitude of failure indices within the joint region. However, The Failure index profiles at different bondline interfaces of the TSLJ subjected to pressure and torsion (Figure 7.4) reveal that introduction of torsion with respect to pressure is tremendously affecting the magnitude of failure indices. The outer adherend-adhesive interface which has been identified as the critical bondline interface for both pure pressure and pure torsional loading has also been observed to be the layer with maximum failure indices for the case of combined pressure and torsional loading. However, the failure prone region is towards the clamped edge of the bonded TSLJ under combined pressure and torsional loading which again confirms the predominance of the torsional loading.

7.4.3 Effect of torque variation in presence of internal pressure on stresses in the critical bondline interface

As the torque has been varied from 100 N-m to 130 N-m in presence of a constant pressure of 10 MPa, it can be observed that only the shear stress (τθz) component have been increasing prominently. The radial-circumferential shear stress component (τrθ) has been observed to have mild variations with respect to the torque change.

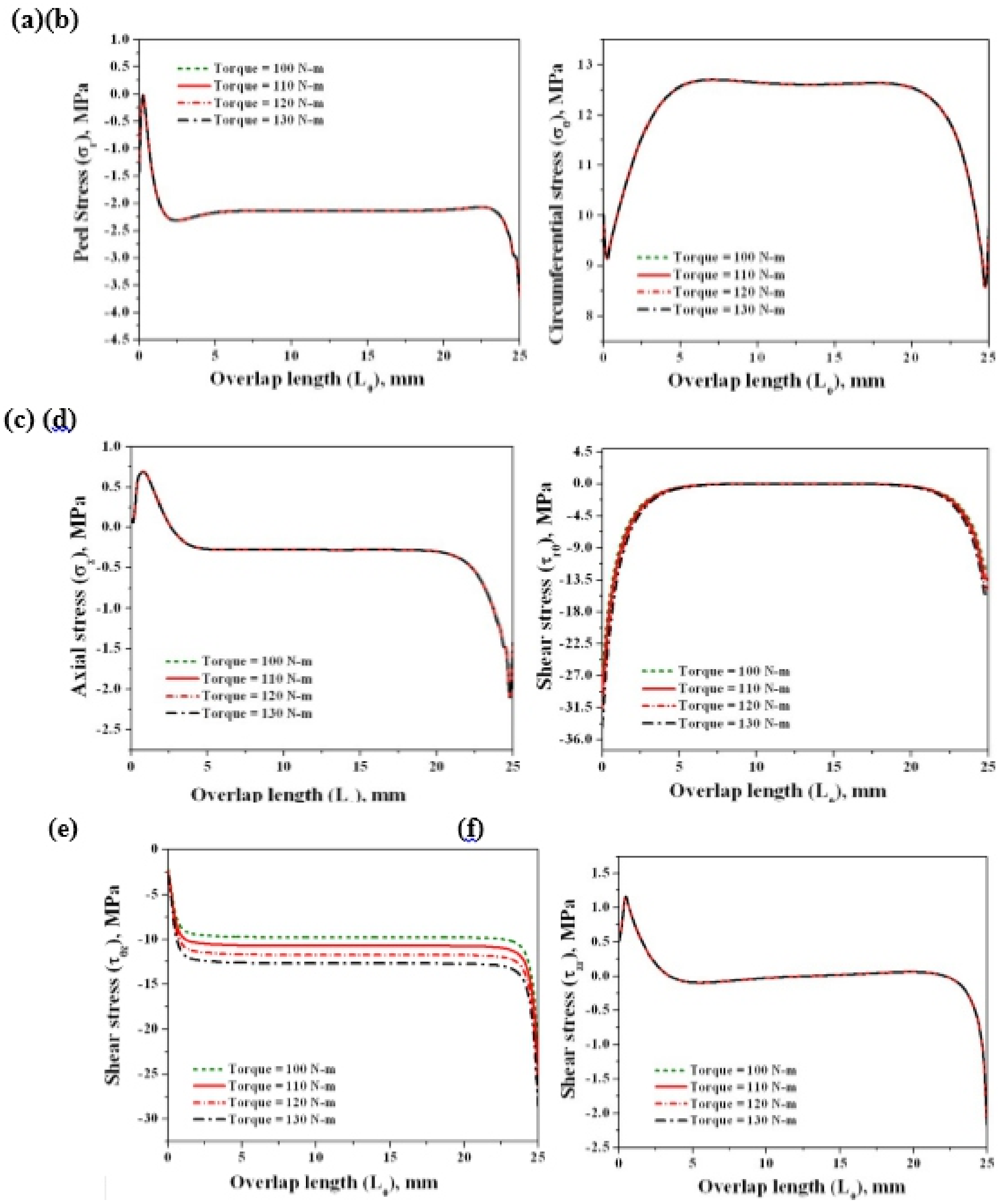

Figure.7.5. Effect of increase in torsional loading in presence of internal pressure on stress distributions within the outer adherend-adhesive interface.

However the remaining shear stress components, τrz) as well as normal stress component (σr, σθ, σz,) has remained unchanged due to the torque variation (Figure 7.5).

7.4.4 Effect of torque variation in presence of pressure on failure at the critical bondline interface

Although variation of torsion loading at constant pressure has not induce much more impact on the stress distribution at the outer adherend-adhesive interface (Figure 7.5), but it has got a bit effect on the failure index values as shown in Figure (7.6.) So increase in torque has got a little effect on the failure at the critical bondline interface (outer adherend-adhesive interface).

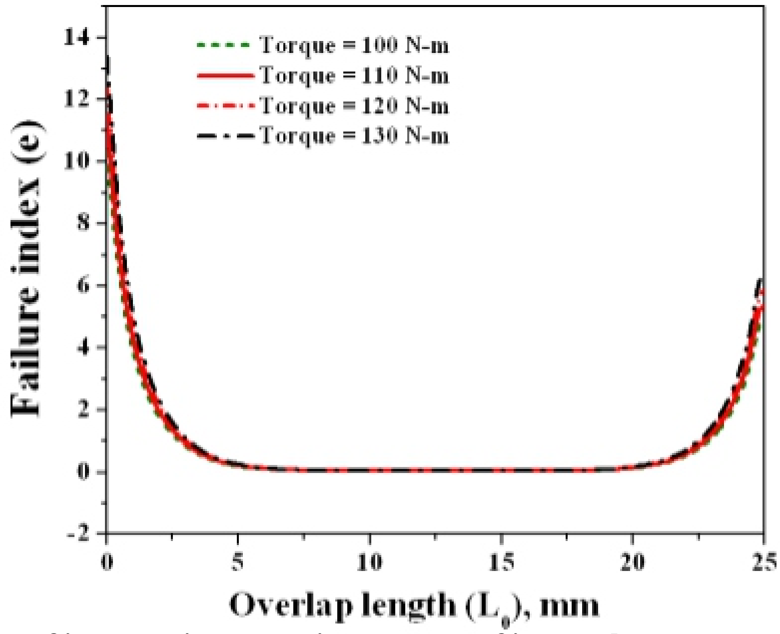

Figure. 7.6 Effect of increase in torque in presence of internal pressure on failure within the outer adherend- adhesive interface.

7.5 Summary and conclusions

Laminated FRP composite made bonded TSLJ subjected to a constant pressure (10 MPa) and varying torsional loading (100 N-m to 130 N-m) has been analyzed through finite element method. The FE codes have been developed through ANSYS APDL in a high speed IBM platform. Stress and failure effects within the joint region have been studied carefully in presence and absence of internal pressure (along with torsional loading). The salient conclusions have been enlisted below.

- Two stress ($\tau r\theta$ and $\tau\theta z$) components within all the bondline interfaces have been enhanced considerably (maintain the same magnitude as in the case of pure torsional loading) due to introduction of torsional loading along with a constant internal pressure.
- However, the remaining stress components (σr, $\sigma\theta$, σz, τrz) remain unaltered (maintain the same magnitude as in the case of pure pressure loading) due to introduction of torsional loading along with a constant internal pressure.
- Introduction of torsional loading along with the pure internal pressure loading is tremendously affecting the failure index profiles at different bondline interfaces of the TSLJ.
- As the torque has been varied, only two stress components ($\tau r\theta$ and $\tau\theta z$) within the joint have been increasing. However, the remaining normal as well as shear stress components (σr, $\sigma\theta$, σz, τrz,) have remained unchanged.
- Increase in torque in presence of constant pressure has got a considerable effect on enhancing the failure indices at the critical bondline interface (outer adherend-adhesive interface).

REFERENCES

1. *Adams, R. D., 2005, Adhesive Bonding: Science Technology and Applications, CRC Press, England.*
2. *Adams, R.D. and Peppiatt, N.A., 1977, "Stress analysis of adhesive bonded lap joints," Journal of Adhesion, 9, pp. 1-18.*
3. *Adams, R. D. and Wake, W. C., 1984, Structural Adhesive Joints in Engineering, Elsevier Science Publishing Company, United Kingdom.*
4. *Chen, D., and Cheng, S., 1992, "Torsional stress in tubular lap joints," International Journal of Solids and Structures, 29, pp. 845-853.*
5. *Cheng, J.C. and Li, G., 2008, "Stress analyses of smart pipe joint integrated with piezoelectric composite layers under torsion loading," International Journal of Solids and Structures, 45, pp. 1153-1178.*
6. *Chon, T.C., 1982," Analysis of tubular lap joint in torsion," Journal of Composite Materials.16, pp. 268-284.*
7. *Das RR, Pradhan B. Int J Adhes 2010 " Adhesion failure analyses of bonded tubular single lap joints in laminated fibre reinforced plastic composites";30:425–38.*
8. *Esmaeel RA, Taheri F. J AdhesSciTechnol 2009 " Influence of adherend's delamination on the response of single lap and socket tubular adhesively bonded joints subjected to torsion";23:1827–44.*
9. *Fu, M. and Mallick, P.K., 2000, "Performance of adhesive joints in an automotive composite structure," Journal of Materials and Manufacturing, Paper No: 2000-01-1131.*
10. *Hashim, S.A., Cowling, M.J. and Lafferty, S., 1998, "Integrity of bonded joints in large composite pipes," International Journal of Adhesion and Adhesives, 18(6), pp. 421-429.*
11. *Huille, A., Yang, C. and Pang, S.S., 1997, "Buckling analysis of thick-walled composite pipe under torsion," Journal of Pressure Vessel Technology, 119(1), pp. 111-121.*
12. *Lubkin, J.L. and Reissner, E., 1958, "Stress distribution and design data for adhesive lap joints between circular tubes," ASME Transactions: Journal of Applied Mechanics, 78, pp.1213-1221.*

Instructions for Authors

Essentials for Publishing in this Journal

1 Submitted articles should not have been previously published or be currently under consideration for publication elsewhere.

2 Conference papers may only be submitted if the paper has been completely re-written (taken to mean more than 50%) and the author has cleared any necessary permission with the copyright owner if it has been previously copyrighted.

3 All our articles are refereed through a double-blind process.

4 All authors must declare they have read and agreed to the content of the submitted article and must sign a declaration correspond to the originality of the article.

Submission Process

All articles for this journal must be submitted using our online submissions system. http://enrichedpub.com/ . Please use the Submit Your Article link in the Author Service area.

Manuscript Guidelines

The instructions to authors about the article preparation for publication in the Manuscripts are submitted online, through the e-Ur (Electronic editing) system, developed by **Enriched Publications Pvt. Ltd**. The article should contain the abstract with keywords, introduction, body, conclusion, references and the summary in English language (without heading and subheading enumeration). The article length should not exceed 16 pages of A4 paper format.

Title

The title should be informative. It is in both Journal's and author's best interest to use terms suitable. For indexing and word search. If there are no such terms in the title, the author is strongly advised to add a subtitle. The title should be given in English as well. The titles precede the abstract and the summary in an appropriate language.

Letterhead Title

The letterhead title is given at a top of each page for easier identification of article copies in an Electronic form in particular. It contains the author's surname and first name initial .article title, journal title and collation (year, volume, and issue, first and last page). The journal and article titles can be given in a shortened form.

Author's Name

Full name(s) of author(s) should be used. It is advisable to give the middle initial. Names are given in their original form.

Contact Details

The postal address or the e-mail address of the author (usually of the first one if there are more Authors) is given in the footnote at the bottom of the first page.

Type of Articles

Classification of articles is a duty of the editorial staff and is of special importance. Referees and the members of the editorial staff, or section editors, can propose a category, but the editor-in-chief has the sole responsibility for their classification. Journal articles are classified as follows:

Scientific articles:

1. Original scientific paper (giving the previously unpublished results of the author's own research based on management methods).
2. Survey paper (giving an original, detailed and critical view of a research problem or an area to which the author has made a contribution visible through his self-citation);
3. Short or preliminary communication (original management paper of full format but of a smaller extent or of a preliminary character);
4. Scientific critique or forum (discussion on a particular scientific topic, based exclusively on management argumentation) and commentaries. Exceptionally, in particular areas, a scientific paper in the Journal can be in a form of a monograph or a critical edition of scientific data (historical, archival, lexicographic, bibliographic, data survey, etc.) which were unknown or hardly accessible for scientific research.

Professional articles:

1. Professional paper (contribution offering experience useful for improvement of professional practice but not necessarily based on scientific methods);
2. Informative contribution (editorial, commentary, etc.);
3. Review (of a book, software, case study, scientific event, etc.)

Language

The article should be in English. The grammar and style of the article should be of good quality. The systematized text should be without abbreviations (except standard ones). All measurements must be in SI units. The sequence of formulae is denoted in Arabic numerals in parentheses on the right-hand side.

Abstract and Summary

An abstract is a concise informative presentation of the article content for fast and accurate Evaluation of its relevance. It is both in the Editorial Office's and the author's best interest for an abstract to contain terms often used for indexing and article search. The abstract describes the purpose of the study and the methods, outlines the findings and state the conclusions. A 100- to 250-Word abstract should be placed between the title and the keywords with the body text to follow. Besides an abstract are advised to have a summary in English, at the end of the article, after the Reference list. The summary should be structured and long up to 1/10 of the article length (it is more extensive than the abstract).

Keywords

Keywords are terms or phrases showing adequately the article content for indexing and search purposes. They should be allocated heaving in mind widely accepted international sources (index, dictionary or thesaurus), such as the Web of Science keyword list for science in general. The higher their usage frequency is the better. Up to 10 keywords immediately follow the abstract and the summary, in respective languages.

Acknowledgements

The name and the number of the project or programmed within which the article was realized is given in a separate note at the bottom of the first page together with the name of the institution which financially supported the project or programmed.

Tables and Illustrations

All the captions should be in the original language as well as in English, together with the texts in illustrations if possible. Tables are typed in the same style as the text and are denoted by numerals at the top. Photographs and drawings, placed appropriately in the text, should be clear, precise and suitable for reproduction. Drawings should be created in Word or Corel.

Citation in the Text

Citation in the text must be uniform. When citing references in the text, use the reference number set in square brackets from the Reference list at the end of the article.

Footnotes

Footnotes are given at the bottom of the page with the text they refer to. They can contain less relevant details, additional explanations or used sources (e.g. scientific material, manuals). They cannot replace the cited literature.
The article should be accompanied with a cover letter with the information about the author(s): surname, middle initial, first name, and citizen personal number, rank, title, e-mail address, and affiliation address, home address including municipality, phone number in the office and at home (or a mobile phone number). The cover letter should state the type of the article and tell which illustrations are original and which are not.

Note